UNITED NATIONS EDUCATIONAL, SCIENTIFIC AND CULTURAL ORGANIZATION
INTERNATIONAL ATOMIC ENERGY AGENCY
INTERNATIONAL CENTRE FOR THEORETICAL PHYSICS
I.C.T.P., P.O. BOX 586, 34100 TRIESTE, ITALY, CABLE: CENTRATOM TRIESTE

H4.SMR/984-8

Winter College on Quantum Optics: Novel Radiation Sources

3-21 March 1997

Pulse matching

E. Arimondo

Dipartimento di Fisica, Università degli Studi di Pisa, Italy

ELSEVIER

1 June 1996

Optics Communications 127 (1996) 55–61

OPTICS COMMUNICATIONS

Matched pulses and electromagnetically induced transparency for the interaction of laser pulse pairs with a double-vee system

Elena Cerboneschi [a], Ennio Arimondo [b,1]

[a] *Dipartimento di Fisica, Università di Pisa, Piazza Torricelli 2, I-56126 Pisa, Italy*

[b] *JILA, University of Colorado, Boulder, CO 80309-0440, USA*

Received 20 September 1995; revised version received 23 January 1996; accepted 24 January 1996

Abstract

We demonstrate the occurrence of electromagnetically induced transparency with pulse matching in the propagation of two probe pulses through a double-vee (DV) system prepared by a pair of strong coupling fields. Pulse matching is connected to the phenomenon of coherent population trapping. We show that the space–time evolution of the probe pulses is determined by a pair of normal modes that describe the propagation of the pulsed excitation through the medium. The establishment of the pulse-matching propagation regime and the transparency for the probe pulses are related to the absorption properties of the normal modes.

PACS: 42.50.Gy; 42.25.Bs; 42.50.Hz

1. Introduction

Electromagnetically induced transparency (EIT) consists of a modification of the absorption and dispersion properties of an absorbing medium produced by an electromagnetic field and allows the propagation of a second field with reduced losses [1–3]. EIT depends on the creation of atomic coherences and the occurrence of interferences in the absorption process. Coherent bleaching in the interaction of cw electromagnetic fields with Λ and double-Λ (DΛ) level systems [4] is a precursory achievement in this field. Dressed fields [5] and adiabatons [6] evidence different EIT features in the shape-preserving propagation of optical pulses. Recently, the first experimental description of the temporal and spatial behaviour of propagating EIT pulses was reported [7].

In the context of EIT, matched pulses have been predicted theoretically in the interaction of copropagating optical pulse pairs with three-level atoms in Λ or cascade configurations [8–11]. In these level schemes, pulse matching is related to coherent population trapping (CPT) [12]. The field envelopes of matched pulses have a definite ratio of intensity and phase, determined by the quantum preparation of the atomic system in the CPT state, and have a space–time profile specified by the input pulse shapes. Matched pulses propagate without losses and without group velocity dispersion.

We have recently demonstrated that pulse matching is conveniently achieved in the DΛ scheme with a pair of coupling pulses preparing the atomic system and a pair of probe pulses showing pulse match-

[1] Permanent address: Dipartimento di Fisica, Universitá di Pisa, Piazza Torricelli 2, I-56126 Pisa, Italy.

0030-4018/96/$12.00
PII S0030-4018(96)00058-2

Reprinted from

PROGRESS IN OPTICS

VOLUME XXXV

EDITED BY

E. WOLF
University of Rochester, N.Y., U.S.A.

Contributors

E. ARIMONDO, J. BERNARD, R. BROWN, Ts. GANTSOG, K. ITOH, B. LOUNIS, A. MIRANOWICZ, M. ORRIT, D. PAOLETTI, N. N. ROSANOV, G. SCHIRRIPA SPAGNOLO, R. TANAŚ

1996

ELSEVIER
AMSTERDAM · LAUSANNE · NEW YORK · OXFORD · SHANNON · TOKYO

E. WOLF, PROGRESS IN OPTICS XXXV

V

COHERENT POPULATION TRAPPING IN LASER SPECTROSCOPY

BY

E. ARIMONDO*

JILA,
University of Colorado at Boulder,
Boulder, CO 80309-0440, USA

* JILA Visiting Fellow 1994–1995. Permanent address: Dipartimento di Fisica dell'Università di Pisa, Piazza Torricelli 2, 56126 Pisa, Italy.

CONTENTS

This article is dedicated to the memory of A. Gozzini and G.W. Series, great teachers in atomic spectroscopy.

§ 1. Introduction

Spectroscopic investigations of atoms and molecules are based on the interaction of near-resonant radiation with the species under investigation. The use of monochromatic, intense, and continuously tunable radiation sources, permits very high sensitivity and accuracy to be attained in the determination of the atomic or molecular levels. Although the attention of spectroscopists was restricted to two-level systems for a long time, the possibility of irradiating samples by several electromagnetic fields simultaneously has produced multiphoton transitions and other nonlinear phenomena, whose application has been explored in the continuously expanding field of nonlinear spectroscopy. In comparison to the two-level system, the three-level system, interacting with two monochromatic radiation fields, represents a configuration in which the nonlinear phenomena are greatly enhanced both in the number of possible laser configurations and in the magnitude of the nonlinearities. The development of monochromatic and tunable laser sources has produced a large variety of high-resolution spectroscopic investigations on three-level systems.

Among the different nonlinear processes associated with the three-level atomic systems, the application of two continuous wave radiation fields leads to the preparation of the atom in a coherent superposition of states, which is stable against absorption from the radiation field. This phenomenon has been designated as coherent population trapping, to indicate the presence of a coherent superposition of the atomic states and the stability of the population. Coherent population trapping may be also described as the pumping of the atomic system in a particular state, the coherent superposition of the atomic states, which is a nonabsorbing state. The exciting radiation creates an atomic coherence such that the atom's evolution is prepared exactly out of phase with the incoming radiation and no absorption takes place. This phenomenon was observed for the first time by Alzetta, Gozzini, Moi and Orriols [1976], as a decrease in the fluorescent emission in a laser optical pumping experiment on sodium atoms, involving a three-level system with two ground levels and one excited level. In that experiment, because an inhomogeneous magnetic field was applied along the sodium cell axis, the nonabsorption was produced in only a small region inside the cell, and the phenomenon appeared as a dark line inside

the bright fluorescent cell. As a consequence, names such as dark resonance or nonabsorption resonance have been used in the literature to describe coherent population trapping. At the same time, and independently, the pumping and trapping originated by two laser fields resonant with two coupled transitions was investigated theoretically for three levels in cascade by Whitley and Stroud [1976], and experimentally in sodium atoms with two ground levels and one excited level by Gray, Whitley and Stroud [1978]. The theoretical analyses by Arimondo and Orriols [1976] and Gray, Whitley and Stroud [1978], pointed out that the sodium atoms were pumped in a nonabsorbing state because of the presence of interfering processes. Population trapping during laser-induced molecular excitation and dissociation was examined theoretically by Stettler, Bowden, Witriol and Eberly [1979]. The title of a paper by Gray, Whitley and Stroud [1978] contains, for the first time, the term *coherent trapping*, and in the conclusion of the paper, the phenomenon is defined as a coherent trapping of a population. The complete designation of coherent population trapping appeared for the first time in the abstract of a paper by Agrawal [1981] on the possibilities of using three-level systems for optical bistability. Then the title of a work by Dalton and Knight [1982a] contained the full designation of coherent population trapping with evidence on the main characteristic of the phenomenon.

The process remained a sort of amusing scientific curiosity for some time. If one resonant laser beam is switched on inside a sodium cell, some very bright fluorescence is emitted by the cell. If a second laser beam is sent into the cell, this second laser being slightly detuned from the first one but also in near resonance with the sodium atoms, it produces its own bright fluorescence. The simultaneous application of the two lasers produces coherent population trapping and eliminates the sodium bright fluorescence. This interference effect, produced by the presence of atomic coherence, appears at the macroscopic level. Coherences between states of a quantum-mechanical system are generated whenever an interaction or measurement leaves the system in a linear superposition of the energy eigenstates defined in the absence of the field. Interferences produced by the presence of coherences have been known since the development of quantum mechanics, and their creation has been largely exploited in spectroscopy and quantum optics. However, a macroscopic effect such as the total suppression of fluorescence emission by coherent population trapping is quite unusual.

In the early 1980s some theoretical attention was given to the process of coherent population trapping, with extensions to the case in which the upper state of the three-level system lies in the continuum, e.g., Knight [1984]. However, the

real rise in interest waited for the extensions or applications on the experimental side. The first application, to metrology, is linked to the work by Tench, Peuse, Hemmer, Thomas, Ezekiel, Leiby Jr, Picard and Willis [1981], and Thomas, Hemmer, Ezekiel, Leiby Jr, Picard and Willis [1982] (see also discussion in Knight [1982]), who demonstrated how very high-frequency accuracy in the measurement of the sodium ground-state hyperfine splitting could be obtained by using what they called Ramsey fringes in Raman three-level transitions. That now should be defined as a Ramsey fringe investigation of coherent population trapping. The next application was to optical bistability; Walls and Zoller [1980] investigated theoretically the optical bistability from three-level atoms contained in an optical cavity and driven into the coherent-trapping superposition. That optical bistability was observed for the first time by Mlynek, Mitschke, Deserno and Lange [1982]. After those early observations, the phenomenon of coherent population trapping has been exploited in very different applications: in high-resolution spectroscopy, laser multiphoton ionization, four-wave mixing, and laser-induced structures in the continuum. Increased attention is due to the work of Aspect, Arimondo, Kaiser, Vansteenkiste and Cohen-Tannoudji [1988] on the application of velocity-selective coherent population trapping to laser cooling. Very soon other interesting phenomena such as adiabatic transfer, lasing without inversion, matched pulse propagation, and photon statistics, strictly connected to the trapping properties of the three-level system, were discovered. It should be noted here that even if some theoretical work has considered the extension to molecular systems, the evidence of coherent population trapping in molecules is still very limited and has been associated with the adiabatic transfer experiments of Gaubatz, Rudecki, Schiemann and Bergmann [1990] and of Dam, Oudejans and Reuss [1990].

For the most important steps in the theoretical understanding of coherent population trapping, Hioe and Eberly [1981], and later Hioe [1983, 1984a, 1984b], have shown a relation with the invariants in the density matrix equations: coherent population trapping is related to the SU(3) group symmetries of the Hamiltonian and to some conservation laws satisfied by the density matrix elements of a three-level system during the time evolution. Smirnov, Tumaikin and Yudin [1989] and Tumaikin and Yudin [1990] have presented generalizations in the construction of the coherent population-trapping atomic superposition. Radmore and Knight [1982] and Dalibard, Reynaud and Cohen-Tannoudji [1987] have derived the dressed atom description.

Coherent trapping as an interference phenomenon is closely related to other interference processes well exploited in spectroscopy, such as the Fano windows in the autoionization profile, the level crossing, or the Hanle effect. A strict

connection also exists between coherent population trapping and the weak interaction decay of the K_0 and $\bar{K}_0$ mesons. In coherent population trapping, the two linear superpositions of ground atomic or molecular states present very different lifetimes for the interaction of these superpositions with the radiation field. Owing to weak interaction mixing between the K_0 and $\bar{K}_0$ mesons, their linear superpositions, K_S and K_L, should be considered. Those superpositions have different lifetimes, short and long, with respect to the weak interaction decay. However, it should be noted that the reduction of coherent population trapping to an interference feature is a reductive description: the experimental observations are strongly based on the role played by optical pumping in the atomic preparation into that quantum superposition that presents interference in the absorption or radiative decay.

Coherent population trapping has been examined in several review papers. An early review was presented by Dalton and Knight [1983]. Yoo and Eberly [1985] presented an analysis of the most important theoretical features of the phenomenon, although their attention was devoted to three-level atoms inside an optical cavity. A review by Arimondo [1987] summarized the experimental observations at that time. A more recent review, with more attention toward the theoretical features and the extensions to laser cooling, has been written by Agap'ev, Gornyi and Matisov [1993].

The organization of this chapter is as follows. In § 2 a theoretical introduction presents the basic properties of an atomic system prepared with the coherent population-trapping superposition of states. § 3 deals with several experimental observations concerned with the establishment of coherent trapping in different discrete systems. § 4 very briefly treats the theoretical and experimental aspects of trapping which involves states of the continuum, because a recent review on that subject has been written by Knight, Lauder and Dalton [1990]. The remaining sections are devoted to a review of both the theoretical and experimental features associated with coherent population trapping in laser cooling, adiabatic transfer, lasing without inversion, pulse matching, and photon statistics. The large amount of theoretical work that has been published with respect to the phenomenon and to the constants of motion with relation to the SU(3) symmetry will not be reported here; the book by Shore [1990] and the recent review by Agap'ev, Gornyi and Matisov [1993] deal with most of those features. Nevertheless, § 8 is devoted to the theoretical aspect of coherent population trapping created by spontaneous emission, which is a possibility considered in some theoretical papers. Even if there is little chance of observing the phenomenon, it is presented because of its fundamental connection with coherent population trapping and lasing without inversion.

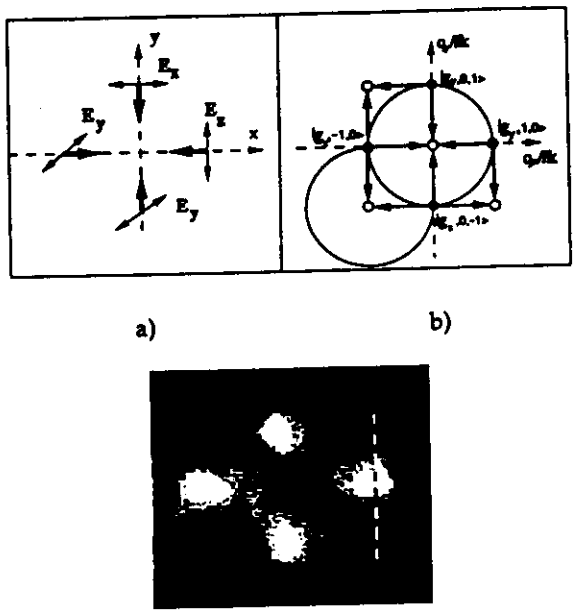

Fig. 24. (a) Schematic diagram of the laser configuration for two-dimensional VSCPT, with counterpropagating lin ⊥ lin laser beams along two directions; (b) solid circles represent the four atomic momentum components, at $\pm\hbar k$ along the two axes, contributing to the noncoupled state, with interfering transitions to excited states (open circles). Circles represent families of states; the wavefunctions of the noncoupled state belong to several families; (c) image of the detected atomic position distribution for VSCPT in two dimensions in ^{4}He, with experimental parameters: $\Omega_R = 0.8\,\Gamma_0$; $\delta_L = 0.5\,\Gamma_0$; interaction time $\Theta = 0.5$ ms. The momentum distribution consists of four peaks as in (b); the peak widths are evidence of a subrecoil two-dimensional VSCPT (from Lawall, Bardou, Saubamea, Shimizu, Leduc, Aspect and Cohen-Tannoudji [1994]).

$J_g = 1 \to J_e = 1$ case, the lin ⊥ lin configuration of counterpropagating lasers in two dimensions, examined by Arimondo [1992], is represented in fig. 24a. Using the selection rules for the linear polarization basis of fig. 7b, the corresponding noncoupled state is obtained as the superposition of $|g_i, q_x, q_y\rangle$ $(i = x, y, z)$ wavefunctions. This is represented schematically in fig. 24b, together with the interference channels in the excitation to upper states. For both σ^+,σ^- and lin ⊥ lin configurations, the wavefunctions composing the noncoupled state do not belong to closed families, so that the efficiency in the preparation of the noncoupled state has not yet been calculated. The configuration of counterpropagating σ^+,σ^- laser fields for VSCPT in two dimensions has been realized by Lawall, Bardou, Saubamea, Shimizu, Leduc, Aspect and Cohen-

Tannoudji [1994] for ^{4}He atoms precooled in a magneto-optical trap using the same $J_g = 1 \rightarrow J_e = 1$ transition of VSCPT in one dimension. After precooling, the helium atoms interacted for 0.5 ms with the four counterpropagating laser beams and were prepared in an noncoupled state similar to that represented in fig. 24b. After the VSCPT cooling, the atoms were falling, due to gravity, onto a CCD camera that recorded an image of the atomic position distribution. Figure 24c shows an image from this camera, with the four spots produced by the detection of the wavefunctions composing the two-dimensional noncoupled state. From the measured width of the individual peaks, as on the vertical profile on the peak at the right of fig. 24c, a temperature around sixteen times smaller than the helium recoil limit was estimated. Examining VSCPT as a function of the laser parameters, the authors deduced the presence of nonspecified laser cooling forces that contribute to the efficiency in the filling of the noncoupled state.

Combinations of linearly and circularly polarized laser fields were examined by Taichenachev, Tumaikin, Yudin and Ol'shanii [1992a,b] for VSCPT on the $J_g = 3/2 \rightarrow J_e = 1/2$ and $J_g = 2 \rightarrow J_e = 1$ transitions.

The idea of atomic states decoupled from the laser field because of quantum interferences was extended by Dum, Marte, Pellizzari and Zoller [1994] to cases in which the electric field amplitudes have a spatial dependence limited in space similar to that of a laser trap, so that the spatial atomic wavefunction also would present a confinement.

§ 6. Adiabatic Transfer

The aim of adiabatic transfer is to transfer an atom or molecule from one lower level of the Λ scheme to the other one by using properly tailored laser pulses, with as large an efficiency as possible. The adiabatic transfer in three- and multilevel systems was investigated theoretically by Oreg, Hioe and Eberly [1984], and Carroll and Hioe [1988]. They demonstrated that by using conditions for the time dependence of the Rabi frequencies $\Omega_{R1}(t)$ and $\Omega_{R2}(t)$ defined as anti-intuitive, a complete transfer of population from level $|1\rangle$ to level $|2\rangle$ is realized. Adiabatic transfer is a consequence of one of the $|NC\rangle$ properties already discussed. From eq. (2.18), $|NC\rangle$ is an eigenstate of the $\mathcal{H}_0 + V_{AL}$ Hamiltonian with zero eigenvalue. If the Hamiltonian is modified adiabatically, so that the system remains in this state, the occupation of the $|NC\rangle$ remains constant. Let us consider a sequence of laser pulses applied to the $|1\rangle \rightarrow |0\rangle$ and $|2\rangle \rightarrow |0\rangle$ transitions, with the time evolution of the electric field amplitudes

described by functions $\Omega_{R1}(t)$ and $\Omega_{R2}(t)$, so that $|NC(t)\rangle$ assumes the following form:

$$|NC(t)\rangle = \frac{\Omega_{R2}(t)}{G}|1\rangle - \frac{\Omega_{R1}(t)}{G}|2\rangle, \tag{6.1}$$

with G given by eq. (2.16b). Adiabatic transfer is realized for a sequence of Rabi frequency time dependencies such as those shown in fig. 25a. If the laser acting on the $|2\rangle \rightarrow |0\rangle$ transition is applied initially, the $|NC\rangle$ state coincides with state $|1\rangle$ where the entire atomic or molecular system is supposed to be concentrated. If the laser acting on the $|2\rangle \rightarrow |0\rangle$ transition is progressively switched off while the laser pulse acting on the $|1\rangle \rightarrow |0\rangle$ transition is switched on (see fig. 25a), eq. (6.1) shows that at the end $|NC(t)\rangle$ coincides with $|2\rangle$, so that in the adiabatic regime the system occupies state $|2\rangle$. The counterintuitive pulse sequence is based on a laser being applied to the second transition at the beginning, and a laser to the first transition at the end. The requirements on the validity of the adiabaticity condition are (Oreg, Hioe and Eberly [1984], Kuklinski, Gaubatz, Hioe and Bergmann [1989], Carroll and Hioe [1990], Band and Julienne [1991a], Shore, Bergmann, Oreg and Rosenwaks [1991], Marte, Zoller and Hall [1991], Shore, Bergmann and Oreg [1992]):

$$\Omega_{R1}, \Omega_{R2} \gg \Gamma_0, \qquad \Omega_{R1}, \Omega_{R2} \gg \frac{1}{T}, \tag{6.2}$$

where T represents the time duration of the two laser pulses. If broad-band lasers are used for the excitation, the spontaneous emission damping rate in the first relation of eq. (6.2) should be replaced by the laser bandwidth, which is equivalent to a damping rate of the optical coherences, as in § 2.8 (He, Kuhn, Schiemann and Bergmann [1990], Kuhn, Coulston, He, Schiemann and Bergmann [1992]).

The first experimental results of adiabatic transfer were obtained on a Na_2 beam with a transfer from the electronic ground and vibrationally excited level $X^1\Sigma_g^+$ ($v=0$, $J=5$) to another vibrational one $X^1\Sigma_g^+$ ($v=5$, $J=5$) using a three-level Λ system with upper electronic excited level $A^1\Sigma_u^+$ ($v=7$, $J=6$) (Gaubatz, Rudecki, Becker, Schiemann, Külz and Bergmann [1988], Kuklinski, Gaubatz, Hioe and Bergmann [1989], Gaubatz, Rudecki, Schiemann and Bergmann [1990]). The counterintuitive time-dependent pulse sequence was created using the time-dependent interaction of sodium molecules crossing c.w. laser beams with separate excitations by the two lasers at different positions along the beam axis. That separated excitation modified drastically the amount of the population transferred to the final state, such as for the realization of

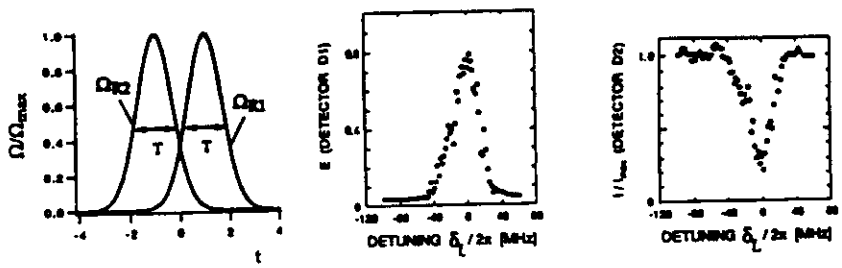

a) b) c)

Fig. 25. (a) Schematic representation of the time dependence for the Rabi frequencies required for adiabatic transfer from level |1⟩ to level |2⟩; (b) experimental results for the adiabatic transfer efficiency between the $X^1\Sigma_g^+$ ($v=0$, $J=5$) and $X^1\Sigma_g^+$ ($v=5$, $J=5$) levels of Na_2 molecules versus the laser 2 frequency, with laser 1 in resonance, and the temporal pulse sequence which maximizes the transfer; (c) experimental results for the fluorescence from excited state $A^1\Sigma_u^+$ ($v=7$, $J=6$) involved in the adiabatic transfer showing the resonant decrease associated with coherent population trapping (from Gaubatz, Rudecki, Schiemann and Bergmann [1990]).

the proper pulsed laser sequence. Figure 25b shows experimental results from Gaubatz, Rudecki, Schiemann and Bergmann [1990] for the transfer efficiency at laser fixed positions scanning the frequency of laser 2, with laser in resonance, with a maximum efficiency around 0.8. Figure 25c shows experimental results for the fluorescence from the upper excited state versus the laser 2 frequency. Corresponding to the maximum of the adiabatic transfer, a minimum was obtained in the excited-state population versus laser frequency, as evidence of coherent population trapping. A similar setup for adiabatic transfer was used by Liedenbaum, Stolte and Reuss [1989], and Dam, Oudejans and Reuss [1990] in a molecular beam of ethylene, C_2H_4, in a three-level cascade configuration. A CO_2 laser induced the transition $gs(4,1,3) \rightarrow \nu_7(5,0,5)$, and from there a color center laser induced the transition to $\nu_7+\nu_9(5,1,4)$. Schiemann, Kuhn, Steuerwald and Bergmann [1993] demonstrated a highly efficient and selective population transfer in NO_2 molecules in the electronic ground $X_2\Pi_{1/2}$ state from vibrational level $v=0$ to level $v=6$, using pulsed lasers properly delayed to realize the counterintuitive sequence of fig. 25a. Sussman, Neuhauser and Neusser [1994] have realized the adiabatic transfer on a Λ system of the C_6H_6 molecule, with pulsed lasers in the counterintuitive time sequence, for preparation in a specific rotational state of a vibronic state of that polyatomic molecule. That transfer was detected through the decrease in the population of the excited state in the Λ system, which represents the coherent population-trapping characteristics.

The adiabatic transfer with a continuum as the upper level of the Λ scheme has been examined theoretically by Carroll and Hioe [1992]. Coulston and Bergmann [1992] have examined the modifications in the process produced by the presence of additional levels close to $|0\rangle$ and $|2\rangle$, such as for the vibra-rotational manifolds of molecular states. Band and Julienne [1991b] have considered the adiabatic transfer in a four-level system and demonstrated that a significant population transfer can be achieved, even if a four-level system does not support coherent population-trapping states.

The concept of adiabatic transfer has been extended by Marte, Zoller and Hall [1991] to the case of noncoupled entangled states involving atomic momentum, such as those involved in the VSCPT processes [see eqs. (5.5) and (5.17)]. For a three-level $J_g = 1 \rightarrow J_e = 1$ atom interacting with two counterpropagating σ^+/σ^- laser beams, such that the linear superposition of eq. (5.5) describes the noncoupled state, the counterintuitive application of a σ^+,σ^- sequence will transfer an atom from the initial $|g_{-1}, p - \hbar k\rangle$ state to the final $|g_{+1}, p + \hbar k\rangle$ state with a modification of the atomic momentum by two times $\hbar k$. For a higher J transition, such as $J_g = 2 \rightarrow J_e = 2$ with the noncoupled state given by eq. (5.17), the adiabatic transfer produces a larger coherent and selective modification of the atomic momentum by $4\hbar k$. The adiabaticity conditions for the photon momentum transfer are those of eq. (6.2), and are quite easily satisfied. Theoretical analyses for alkali atoms have been performed by Weitz, Young and Chu [1994a], and Foot, Wu, Arimondo and Morigi [1994]. The adiabatic transfer between the entangled states of internal and momentum variables has been realized experimentally by different groups. Pillet, Valentin, Yuan and Yu [1993], Goldner, Gerz, Spreeuw, Rolston, Westbrook, Phillips, Marte and Zoller [1994a,b], and Valentin, Yu and Pillet [1994] have demonstrated, using the D_2 excitation of cesium atoms precooled by sub-Doppler techniques, a momentum transfer up to $8\hbar k$ between the extreme Zeeman sublevels of the $F = 4$ hyperfine level, with an efficiency up to 0.5. The off-resonant transitions to other excited states of the $3^2P_{3/2}$ manifold limited the efficiency, which should be larger using the D_1 excitation to the $6^2P_{1/2}$ manifold where the hyperfine separation is larger. Lawall and Prentiss [1994] realized the adiabatic transfer on ^{4}He metastable atoms in a beam using the $2^3S_1 \rightarrow 2^3P_0$ transition, with an efficiency of transfer up to 0.9 for a change of atomic momentum by $2\hbar k$. Using multiple interaction of the lasers with the atomic beam, Lawall and Prentiss [1994] obtained momentum changes up to $6\hbar k$. An immediate application is in atomic interferometry with the adiabatic transfers used as atomic beam splitters. In fact, an atomic interferometer based on adiabatic transfer between the cesium $6^2S_{1/2}$ hyperfine states $|F = 3,\ m_F = 0\rangle$ and $|F = 4,\ m_F = 0\rangle$ using a

σ^+,σ^- polarization configuration has been demonstrated by Weitz, Young and Chu [1994b]. Using the D_1 excitation, a coherent transfer of 140 photon momenta to cesium atoms with an efficiency of 0.95 per exchanged photon was reported.

§ 7. "Lasing Without Inversion"

The idea of lasing without inversion was developed independently by two groups in Russia and the United States, Kocharovskaya and Khanin [1988] and Scully, Zhu and Gavrielides [1989], respectively. The aim is to produce a laser system where the population in the excited atomic, or molecular, state is smaller that the population in the lower state. The states without inversion are defined according to the atomic, or molecular, basis, in the absence of applied radiation fields. Much attention has been given to the subject, both theoretically and experimentally, due to the attractive possibility of converting a coherent low-frequency input into a coherent high-frequency output, without any requirement on population inversion between the high-frequency emitting levels. At the present stage, several mechanisms giving rise to the phenomenon of "lasing without inversion" have been identified, as seen in the reviews by Kocharovskaya [1992] and Scully [1992]. One of those mechanisms has been based on coherent population trapping, and up to now the large majority of the experimental verifications of amplification without inversion is based on this phenomenon. In effect, this mechanism of "lasing without inversion" should be classified as an inversion in the hidden basis of the coupled/noncoupled states. This mechanism of "lasing without inversion" (or more precisely, amplification without inversion (AWI), because a cavity is required to convert an amplifier into a laser), can be easily analyzed when the transformation from the atomic basis $\{|1\rangle, |2\rangle, |0\rangle\}$ to the coherent-trapping basis $\{|NC\rangle, |C\rangle, |0\rangle\}$ is applied, as in fig. 26 (Kocharovskaya, Mauri and Arimondo [1991], Kocharovskaya, Mauri, Zambon and Arimondo [1992]). For the coupled/noncoupled basis, the interaction of the atoms with the externally applied electric field acts only on the $|C\rangle$ and $|0\rangle$ states. In a system at thermal equilibrium, the states $|1\rangle$ and $|2\rangle$ are equally populated, as represented schematically in fig. 26a, and the excited state $|0\rangle$ contains a small population. The population of the $|C\rangle$ state may be transferred to the $|NC\rangle$ state through one of the appropriate mechanisms for creating coherent population trapping already described in this review, or one of those to be discussed later in this section. Perfect coherent population trapping is realized with $\rho_{C,C} \simeq 0$, and an efficient trapping corresponds to $\rho_{NC,NC} \gg \rho_{C,C}$, as shown

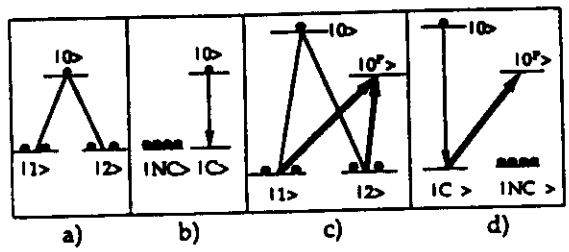

Fig. 26. (a) and (b) Energy levels for amplification without inversion for the Λ scheme, and (c) and (d) for the double-Λ scheme. In (a) and (c) the bare atomic basis is used, and in (b) and (d) the coupled/noncoupled basis is used. The depopulation pumping between coupled and noncoupled levels is schematically represented by the transfer of the black dots.

in fig. 26b. In these conditions, if a population inversion is realized between the levels $|0\rangle$ and $|C\rangle$; i.e.,

$$\rho_{0,0} \gg \rho_{C,C}, \tag{7.1}$$

an amplification of the radiation on the $|0\rangle \rightarrow |C\rangle$ transition could be obtained. This amplification is produced by an inversion between states $|0\rangle$ and $|C\rangle$ in the atomic basis of coupled/noncoupled states, but in the atomic basis of bare states $\{|1\rangle, |2\rangle, |0\rangle\}$ no population inversion exists, because $\rho_{1,1} + \rho_{2,2} = \rho_{C,C} + \rho_{NC,NC} \gg \rho_{0,0}$! This simple presentation exemplifies the concept of amplification in a hidden basis, the basis of the coupled/noncoupled states.

The possibility of obtaining gain in a Λ system on the condition of coherent population trapping is also understood by examining the plot of $\mathrm{Im}(\rho_{01})$, proportional to the absorption coefficient, as shown in fig. 2c, with the very narrow peak at the center which has been defined as electromagnetic-induced transparency (Kocharovskaya [1992], Scully [1992]). By pumping a small amount of the population into the excited state $|0\rangle$, a contribution with opposite sign is added to the absorption coefficient, which could bring that peak above the horizontal axis and create a condition of amplification.

If the condition $\rho_{0,0} \gg \rho_{C,C}$ corresponds to AWI, the operation of a laser requires three levels inside a cavity with the gain larger than the cavity losses. It should be noted that the amplification on the coupled/noncoupled basis corresponds to an amplification of a bichromatic field, i.e., two electromagnetic field waves with frequencies ω_{L1} and ω_{L2}, equal to the two transitions $|0\rangle \rightarrow |1\rangle$ and $|0\rangle \rightarrow |2\rangle$ in the bare atomic basis. If the two frequencies have the same cavity loss κ, and the two optical transitions of the three-level system have

the same absorption coefficient α, the condition for lasing is a straightforward application of the condition for lasing based on a two-level system:

$$\rho_{00} - \rho_{C,C} \geqslant \frac{2\kappa}{\alpha L}, \tag{7.2}$$

where L is the length of the cavity, supposed to be filled uniformly with the three-level medium, presenting amplification without inversion.

The condition of amplification, or more precisely of no absorption, is valid only with respect to the $|NC\rangle$, $|C\rangle$ states of eqs. (2.16), as determined by the process that has prepared those states. In order to realize amplification of a bichromatic electromagnetic field, composed of two different components $\mathcal{E}_{L1}\exp[-i(\omega_{L1}t+\phi_{L1})]$ and $\mathcal{E}_{L2}\exp[-i(\omega_{L2}t+\phi_{L2})]$, the $|NC\rangle$ state should really be noncoupled for that amplified field. As a consequence, the atomic amplitudes and the amplitudes of the electric field components to be amplified by the noninverted medium, should satisfy a matching condition. If the $|1\rangle$ and $|2\rangle$ levels are degenerate in energy, the amplified field has only one frequency component, and the separation between the two modes of the electric field originates from polarization selection rules. On the contrary, if $|1\rangle$ and $|2\rangle$ are separated in energy, the amplified bichromatic field has components at two different frequencies ω_{L1} and ω_{L2}. In this scheme, defined by Fill, Scully and Zhu [1990] as a quantum beat laser, the beat frequency $\omega_{L1} - \omega_{L2}$ should match the evolution frequency of the ground state coherence. Amplification of a bichromatic field also imposes a phase matching condition: in a laser cavity, neglecting cavity losses and frequency pulling with respect to the interaction with the three-level system, the laser field relative phase should be opposite to that of the ground-state coherence. Fill, Scully and Zhu [1990] have derived, for different schemes of creation of the coherent population trapping, the phase-matching equation to be satisfied by the relative phase $\phi_{L1} - \phi_{L2}$ of the two lasers.

The relation (2.20) between the density matrix elements in the coupled/noncoupled basis and in the bare atomic basis shows, that in order to have a small value of $\rho_{C,C}$, the occupation of the noncoupled state, the atomic coherence $|\rho_{12}|$ should be large. The different applications of coherent population trapping for lasing without inversion, both theoretically and experimentally, are really connected to the differences in the preparation of a large atomic coherence ρ_{12} with a small occupation of the $|C\rangle$ state and a large occupation of the $|NC\rangle$ state. An efficient process for the realization of amplification without inversion is based on the double-Λ scheme, as shown in fig. 26c, with the two lower levels, $|1\rangle$ and $|2\rangle$ connected by dipole transitions to the upper levels $|0\rangle$ and $|0^p\rangle$ (Fill, Scully and Zhu [1990], Kocharovskaya, Li and

Mandel [1990], Kocharovskaya and Mandel [1990], Khanin and Kocharovskaya [1990], Kocharovskaya, Mauri and Arimondo [1991], Kocharovskaya, Mauri, Zambon and Arimondo [1992]). A pump bichromatic laser field, with amplitudes $\mathcal{E}_{L1}^{P}\exp[-i\phi_{L1}^{P}]$ and $\mathcal{E}_{L2}^{P}\exp[-i\phi_{L2}^{P}]$ resonant with the $|1\rangle \rightarrow |0^{P}\rangle$ and $|2\rangle \rightarrow |0^{P}\rangle$ transitions to the pumping level $|0^{P}\rangle$, prepares the coherent trapping superposition in the ground state, so that an amplification of a bichromatic field from state $|0\rangle$, with amplitudes $\mathcal{E}_{L1}\exp(-i\phi_{L1})$ and $\mathcal{E}_{L2}\exp(-i\phi_{L2})$, takes place. The preparation of the $|C^{P}\rangle$ and $|NC^{P}\rangle$ states, shown in fig. 26d, takes place through the depopulation pumping process, as discussed in § 2.3, with coupled and noncoupled states given by:

$$|NC^{P}\rangle = \frac{1}{\sqrt{\left|\mu_{0^{P}1}\mathcal{E}_{L1}^{P}\right|^{2} + \left|\mu_{0^{P}2}\mathcal{E}_{L2}^{P}\right|^{2}}}\left(\mu_{0^{P}2}\mathcal{E}_{L2}^{P}e^{-i\phi_{L2}^{P}}|1\rangle - \mu_{0^{P}1}\mathcal{E}_{L1}^{P}e^{-i\phi_{L1}^{P}}|2\rangle\right),$$

$$|C^{P}\rangle = \frac{1}{\sqrt{\left|\mu_{0^{P}1}\mathcal{E}_{L1}^{P}\right|^{2} + \left|\mu_{0^{P}2}\mathcal{E}_{L2}^{P}\right|^{2}}}\left(\mu_{0^{P}1}\mathcal{E}_{L1}^{P}e^{-i\phi_{L1}^{P}}|1\rangle + \mu_{0^{P}1}\mathcal{E}_{L2}^{P}e^{-i\phi_{L2}^{P}}|2\rangle\right). \tag{7.3}$$

However, these coupled and noncoupled states should coincide with those on the transitions to the $|0\rangle$ state, so that the following self-consistent condition between the amplitudes of all the fields applied to the double-Λ system should be satisfied:

$$\frac{\mu_{01}\mathcal{E}_{L1}\exp(-i\phi_{L1})}{\mu_{02}\mathcal{E}_{L2}\exp(-i\phi_{L2})} = \frac{\mu_{0^{P}1}\mathcal{E}_{L1}^{P}\exp(-i\phi_{L1}^{P})}{\mu_{0^{P}2}\mathcal{E}_{L2}^{P}\exp(-i\phi_{L2}^{P})}. \tag{7.4}$$

Kocharovskaya and Mandel [1990] have derived the conditions for the realization of steady-state AWI in the double-Λ scheme taking into account the simultaneous interaction of the four-level system with the two pairs of bichromatic fields. The important condition to be satisfied for the realization of this AWI was that the population of the lasing level $|0\rangle$ should be larger than that of the pumping level $|0^{P}\rangle$. More precisely, the following condition results:

$$\rho_{0,0} - \rho_{0^{P},0^{P}} > \frac{\Gamma_{21}}{\Gamma_{0^{P}}}. \tag{7.5}$$

This relation states than in order to obtain AWI, a population inversion should be realized between the two upper levels, but of course no population inversion is required between these levels and the ground ones. The relation derives from the competition in the creation of coherent population trapping between the two separate Λ schemes of the double Λ. In fact, the population in the

$|0^P\rangle$ state contributes through spontaneous emission or one-photon processes to the pumping of the population in the coupled state $|C\rangle$, whose presence decreases the amplification and increases the threshold of amplification without inversion. In the case of generation of short-wavelength radiation by pumping with a longer wavelength laser, level $|0\rangle$ is higher in energy than level $|0^P\rangle$, and in thermodynamic equilibrium the population of the $|0\rangle$ top level is smaller than that of the $|0^P\rangle$ intermediate level. Thus, the above threshold condition (7.5) cannot be satisfied without external pumping.

The above discussion points out the close equivalence between the double-Λ scheme and a four-level laser. In fact, optical pumping in a four-level system represents an alternative way to realize amplification on the same double-Λ scheme without creation of coherences. For instance, on the same level structure of fig. 26c, pumping from the $|2\rangle$ state to the $|0^P\rangle$ state followed by spontaneous emission down to the $|1\rangle$ level could produce an inversion between $|0\rangle$ and $|2\rangle$. The threshold condition required for amplification on this optical pumping scheme is exactly equivalent to those for AWI in the double Λ (Kocharovskaya, Mauri, Zambon and Arimondo [1992], Fleischhauer and Scully [1994]). These last authors also pointed out that schemes combining optical pumping with the creation of coherences could produce a further reduction of the threshold.

An alternative way to create a lower-state coherence is through the application of a microwave field resonant with the lower-state splitting, as shown schematically in fig. 27a (Scully, Zhu and Gavrielides [1989], Fill, Scully and Zhu [1990], Khanin and Kocharovskaya [1990]). The generated lower-state coherence can be expressed through coupled/noncoupled states. Again, for a population of the $|0\rangle$ level larger than that of the coupled state, amplification takes place, with inversion in the basis of the coupled/noncoupled states. The main difference between the double-Λ scheme and the microwave field is that in the double-Λ scheme the depopulation pumping of the coupled state leads to the preparation of a pure density matrix state, i.e., with all the atoms prepared in the noncoupled state. For microwave-generated coherence, starting from the nonpure state of the thermal occupation of ground states, the application of a microwave-coherent field cannot produce a pure state. As a consequence, the gain in the microwave case is always smaller than in the double-Λ scheme. The thermal nonpure occupation of the ground states leads to the following condition for AWI: $\rho_{00} \geqslant \min(\rho_{11}, \rho_{22})$ (Mandel and Kocharovskaya [1993]).

Another scheme for the realization of amplification without inversion, actually the first one proposed by Kocharovskaya and Khanin [1988] and examined later by Fleischhauer, Keitel, Scully and Su [1992], is based on the application to the

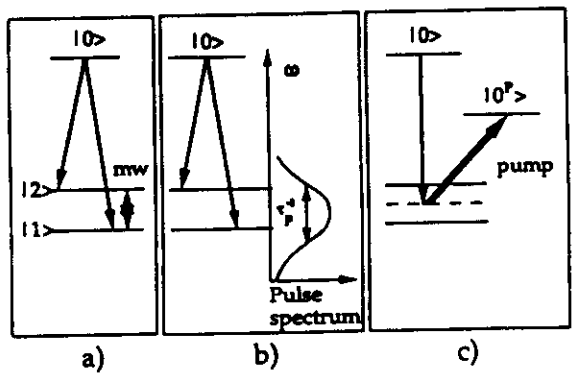

Fig. 27. Additional schemes for amplification without inversion based on coherent population trapping: (a) preparation of the coherent trapping superposition through a microwave field and amplification of the bichromatic field; (b) coherent trapping superposition formed by an ultrashort laser pulse with duration τ_p; (c) four-level scheme with pump laser to the level $|0^P\rangle$ tuned halfway between the ground levels with amplified laser also tuned halfway between ground levels.

three-level system of a short laser pulse, as in fig. 27b and as for the experiments described in § 3.3. In order for the short pulse with temporal duration τ_p to interact with both the ω_{01} and ω_{02} optical transitions and to probe the low-frequency coherence ρ_{21}, the relation $1/\tau_p \gg \omega_{21}$ must be satisfied. As usual, the gain is based on the preparation of a small population in the upper $|0\rangle$ level, with population in the lower states lying in the $|NC\rangle$ state. The $|NC\rangle$ occupation should have been realized before the pulse arrival, by applying a microwave field, using the double-Λ scheme, or by applying a train of pulses as described in § 3.3.

The last scheme involving coherent population trapping, proposed by Narducci, Doss, Ru, Scully, Zhu and Keitel [1991], is based on the combination of the double-Λ scheme and the dressed-state approach of § 2.4 and fig. 5a: a coherent population-trapping preparation is performed on one Λ system and amplification is achieved on the second Λ system, as shown in fig. 27c. Only one laser is required for the preparation stage, and only one laser is used for the amplification process, both lasers being tuned at the center frequency between the two groundstate levels.

The scheme of fig. 27c was tested in the first experiment of inversionless amplification performed on sodium atoms by Gao, Guo, Guo, Jin, Wang, Zhao, Zhang, Jiang, Wang and Jiang [1992], with lower levels being the hyperfine states of $3^2S_{1/2}$ ground level, $3^2P_{3/2}$ as the $|0\rangle$ amplification state, and $3^2P_{1/2}$ as the $|0^P\rangle$ preparation state. In the experiment a discharge through the helium/argon buffer gas prepared the required small occupation in the excited sodium states, and a strong pulsed laser on the $\{|1\rangle, |2\rangle\} \rightarrow |0^P\rangle$ transitions produced the

coherent trapping superposition. The amplification of a c.w. dye laser on the $|0\rangle \rightarrow \{|1\rangle, |2\rangle\}$ transitions was monitored, through a boxcar detector, during the application of the pulsed laser. These authors have reported AWI, and Gao, Zhang, Cui, Guo, Jiang, Wang, Jin and Li [1994] have measured the excited-state population through the absorption of a second c.w. dye laser from the excited state in order to verify that no population inversion in the bare states was created by the strong preparation pulse. The positive result of that experiment has generated some discussion in the lasing-without-inversion community: the possibility of a real population inversion between the excited state and ground states produced by the pulsed laser was ruled out in their direct absorption measurements. Because the experiment was performed in a transient regime, a theoretical analysis of the transient AWI was performed by Doss, Narducci, Scully and Gao [1993], proving that amplification is also reached in the transient regime. A later analysis by Meyer, Rathe, Graf, Zhu, Fry, Scully, Herling and Narducci [1994] showed that no coherence between the ground state hyperfine levels could have been created in that sodium experiment.

Clearer evidence of AWI, based on the scheme of fig. 27c, was obtained by Kleinfeld and Streater [1994] in potassium atoms, using the ground $4^2S_{1/2}$ hyperfine levels, $4^2P_{3/2}$ as the preparation state, and $4^2P_{1/2}$ as the amplifying state. Continuous lasers were used for both preparation and amplification, tuned at the center between the two ground hyperfine states separated by 462 MHz. The upper-state population in the amplifying state was produced making use of the transfer from $4^2P_{3/2}$ to $4^2P_{1/2}$ in collisions between potassium and helium buffer gas. The experimental results were very similar to those predicted in the theoretical analysis by Narducci, Doss, Ru, Scully, Zhu and Keitel [1991], with some unexplained features of additional absorption dips just outside the gain peaks.

In the experiments by Nottelman, Peters and Lange [1993] and by Lange, Nottelman and Peters [1994], a coherent population trapping in the ground state of a Λ scheme was created through a train of picosecond pulses, as shown in fig. 27b and as analyzed in § 3.3. A second picosecond pulse probed, at different delay times, the amplification without inversion. Samarium atoms on the $J_g = 1 \rightarrow J_e = 0$ transition (as in the experiment by Parigger, Hannaford and Sandle [1986] discussed in § 3.5), in the presence of an applied magnetic field along the z axis, were irradiated by a train of 30 ps laser pulses, with electric field polarization along the y axis, a ground-state Hanle-effect configuration. When the matching condition of eq. (3.1) was satisfied, the picosecond pulse-train pumped atoms out of the $|J_g, C\rangle = |J_g = 1, y\rangle$ state and created the $|J_g, NC\rangle \equiv |J_g = 1, x\rangle$ coherent superposition of states, as from the selection

rules of eq. (2.32b). However, in the presence of a magnetic field B, that superposition is not an eigenstate and the atomic wavefunction experiences a time evolution. Because of the energy separation $\omega_{21} = 2g\mu_B B/\hbar$ between the $|J_g, m_J = 1\rangle$ and $|J_g, m_J = -1\rangle$ eigenstates of the atomic Hamiltonian, starting from a perfect atomic preparation at time $t = 0$ in the noncoupled state, the atomic wavefunction $|\psi_g(t)\rangle$ at time t is:

$$|\psi_g(t)\rangle = \cos\frac{\omega_{21}t}{2}\,|\mathrm{NC}\rangle - \sin\frac{\omega_{21}t}{2}\,|\mathrm{C}\rangle\,. \tag{7.6}$$

From eq. (7.6) it can be seen that the absorption from the $|\mathrm{C}\rangle$ part of $|\psi_g(t)\rangle$ varies with the delay time of the probe pulse. At $t_d = \pi/2\omega_{21}$, the occupation of the coupled state is equal to one half the initial value; at $t_d = \pi/\omega_{21}$ the occupation of the coupled state is equal to 1, and it is 0 at $t_d = 2\pi/\omega_{21}$. In order to realize AWI, a third pulse, linearly polarized along the z axis, pumped a few atoms from the ground $|J_g = 1, z\rangle$ state to the $|J_e = 0\rangle$ state, and the amplification between the excited $|J_e = 0\rangle$ state and the $|\mathrm{C}\rangle \equiv |J_g = 1, y\rangle$ state was probed by the delayed pulse. Depending on the delay time, the coupled-state occupation produced different contributions, so that at a proper delay time an inversion between $|J_e = 0\rangle$ and $|J_g = 1, \mathrm{C}\rangle$ could be realized with no population inversion in the Zeeman atomic basis. Actually, the experiment was operated slightly differently from that presented: at a fixed delay time of the probe, the tuning of the occupation of the coupled state was realized by varying the splitting ω_{21} through an applied magnetic field B. Moreover, the maximum value of the generated ground-state coherence was only 0.14, so that the full occupation of the coupled or noncoupled states could not be realized. Finally, while the relatively long decay time of the ground-state coherence (~15 ns) was beneficial for the experiment, the comparable decay time of the optical coherence ($\approx$ 9 ns) implied that the atomic dispersion affected the pulse propagation, and the length of the samarium cell could not be increased. Thus, as stated by the authors, the measured amplification of 7% did not seem exciting, but was obtained with an optically thin sample.

Another experiment by Fry, Li, Nikonov, Padmabandu, Scully, Smith, Tittel, Wang, Wilkinson and Zhu [1993] was based on the sodium D_1 resonance line. A detailed analysis and presentation of the experimental results has been published in a series of four papers: Meyer, Rathe, Graf, Zhu, Fry, Scully, Herling and Narducci [1994], Nikonov, Rathe, Scully, Zhu, Fry, Li, Padmabandu and Fleischhauer [1994], Padmabandu, Li, Su, Fry, Nikonov, Zhu, Meyer and Scully [1994], and Graf, Arimondo, Fry, Nikonov, Padmabandu, Scully and Zhu [1995]. The level configuration involved in this experiment was based on two

σ^+ circularly polarized lasers exciting hyperfine components of the D_1 line and has already been presented in fig. 7f. The two laser beams, with linewidth ≈ 30 MHz and frequency difference matching the 1.77 GHz ground hyperfine splitting, were generated through an acousto-optic frequency shifter. The first step in the experiment was to test the production of the coherent population-trapping superposition by the bichromatic σ^+ radiation: one of the pumping lasers was switched off through a fast Q-switch and the transient absorption of the sodium atoms on the remaining pumping beam, as a consequence the destruction of the coherent trapping was monitored. The time evolution of the transmitted light was in good agreement with theoretical predictions. AWI was realized by pumping atoms to the excited $F=2$ state from the ground $F=2$, $m_F=2$ level not involved in the coherent trapping superposition, through application of a weak excitation σ^- polarized light. As soon as the population inversion was established, an amplification of the bichromatic σ^+ radiation was observed. The amount of coherence established between the ground levels was not specified; however, in a theoretical analysis, which well reproduced the experimental results, a ground-state coherence around 0.10–0.12 was reported. The observed dependence of the coherent trapping superposition on the helium buffer gas has been discussed in § 2.8.

The last experiment in the coherent population-trapping application by van der Veer, van Dienst, Dönszelmann and van Linden van den Heuvell [1993], operated on a cascade scheme based on the ^{112}Cd $5s^2\,{}^1S_0 \rightarrow 5s5p\,{}^3P_1 \rightarrow 5s6s\,{}^3S_1$ levels, with transitions at wavelengths 326 nm and 308 nm. A longitudinal magnetic field B_x in the mT range produced an energy splitting of the excited $^3P_1$ state. Nanosecond-pulsed dye lasers, with frequency bandwidths in the GHz range to match the Doppler-broadening of the absorption lines, counterpropagated through a cadmium cell. The two lasers were linearly polarized, and the preparation, as well as the amplification processes are well understood in the level scheme based on the linearly polarized atomic basis of fig. 28a. Laser 1, linearly polarized along the x axis, excited the cadmium atoms from the $|{}^1S, J_g = 0\rangle$ state to the $|{}^3P_1, x\rangle$ state. Laser 2, linearly polarized along the y axis, transferred atoms to the $|{}^3S_1, z\rangle$ state. From there, amplification could be produced with emission towards the $|{}^3P_1, y\rangle$ state. This interpretation of AWI comes out very naturally in the hidden basis, whereas in the Zeeman atomic basis the interpretation of amplification without inversion requires a careful analysis of the atomic coherences created in the intermediate $^3P_1$ state. The presence of amplification was tested by monitoring the gain of a seed laser transmitted through the cadmium cell, and a gain of 4.3 was measured. The amplification was monitored in two different regimes. In the first one, laser 2

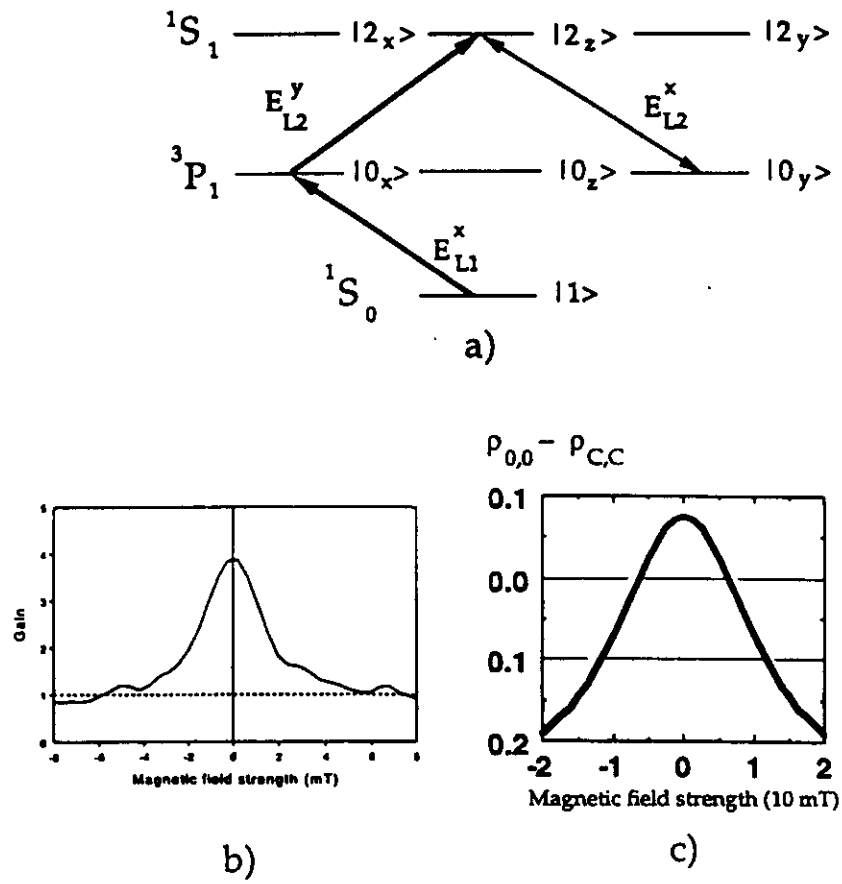

Fig. 28. (a) Level scheme, in the linear atomic basis (see § 2.6), for the ^{112}Cd AWI experiment, and (b) measured AWI gain versus applied magnetic field, with a loss of gain at the larger magnetic field due to the absence of population inversion (from van der Veer, van Dienst, Dönszelmann and van Linden van den Heuvell [1993]); (c) hidden basis population inversion in a ^{87}Rb double-Λ scheme versus an applied magnetic field; spontaneous emission rate $\Gamma_0 = 0.24\,\Gamma_0^p$, pumping rate $0.05\,\Gamma_0^p$ to excited state $|0\rangle$, Rabi frequencies $\Omega_{R1}^p = \Omega_{R2}^p = 0.12\,\Gamma_0^p$, and interaction time for preparation of the coupled/noncoupled state $\Theta = 83\,\Gamma_0^p$ (adapted from Kocharovskaya, Mauri and Arimondo [1991]).

was delayed by 30 ns with respect to laser 1, and when the amplification was measured versus the applied magnetic field, the periodic evolution between the coupled and noncoupled states could be monitored. In the second regime the two lasers produced simultaneous excitation to the top level of the cascade scheme, and the amplification was observed as a function of the magnetic field with

experimental results reported in fig. 28b. Figure 28c reports the results of a theoretical analysis for the population inversion in the hidden basis, proportional to the gain, as a function of the applied magnetic field, derived for the double-Λ scheme of ^{87}Rb atoms in Kocharovskaya, Mauri and Arimondo [1991]. The strong similarity between the two figures evidences the common features of evolution between coupled/noncoupled or $|x\rangle/|y\rangle$ states.

The use of the index of refraction has been considered in the context of amplification without inversion (Scully [1991, 1992], Fleischhauer, Keitel, Scully and Su [1992], Fleischhauer, Keitel, Scully, Su, Ulrich and Zhu [1992], Friedmann and Wilson-Gordon [1993]). It has already been noted (see fig. 2d and § 3.8) that a large index of refraction can be generated in the conditions of coherent population trapping. The use of that large index of refraction could be inhibited by the absorption coefficient of the material, which is large outside of the Raman resonance (see fig. 2c). However, by preparing the three-level system with a small population in the upper $|0\rangle$ state, a contribution to the absorption with opposite sign could be created, which is really an amplification, so that a regime may be realized with the large index of refraction occurring at a laser frequency where the absorption coefficient is effectively equal to zero. Applications of the enhancement of the index of refraction, considered by Scully [1991], are to the realization of phase-matching in the laser acceleration of electrons, to the increase of the resolving power in a microscope, and to the development of a new class of magnetometers. The experiments by Schmidt, Hussein, Wynands and Meschede [1993, 1995] and Xiao, Li, Jin and Gea-Banacloche [1995] on the index of refraction, as discussed in § 3.8, have been performed with the aim of modifying the group velocity for propagation inside a medium pumped so that it gives rise to coherent population trapping. A group velocity $v_g = c/1280$ has been reported by the first group of authors.

Attention here has been concentrated on schemes where no population inversion exists in the basis of the bare atomic states, but a population inversion is found in the basis of coupled/noncoupled states, or equivalently in the basis of dressed states. Other schemes of amplification without inversion have been identified where population inversion does not appear to occur in any basis (Kocharovskaya [1992]). However, the transformation from the bare-atomic basis to the dressed-state basis transforms population differences into coherences, so that the gain can be associated with the creation of coherences (Agarwal [1991a], Bhanu Prasad and Agarwal [1991]). Even if the amplification cannot be described simply through a population inversion in an appropriate basis, the role of coherence population trapping cannot be excluded. For instance, in an asymmetrical Λ scheme with level $|2\rangle$ metastable and the Rabi frequency Ω_{R2}

quite large, AWI can be realized on the $|0\rangle \rightarrow |1\rangle$ transition (Imamoglu, Field and Harris [1991]). For that process, Cohen-Tannoudji, Zambon and Arimondo [1993] pointed out the important role played by coherent population trapping. For $\Omega_{R1} \ll \Omega_{R2}$, the ground state $|1\rangle$ coincides with the noncoupled state, so that even a small population in the $|0\rangle$ state may be able to produce amplification.

Dowling and Bowden [1993] have considered AWI in a dense medium, where the near dipole–dipole interactions modify the local microscopic electric field through volume polarization, as in the Lorenz–Lorentz local field correction. This dipole–dipole interaction also would affect the phenomenon of coherent population trapping in a dense medium, with a frequency shift and a distortion of the resonance lineshapes.

§ 8. Coherences Created by Spontaneous Emission

The possibility of creating ground-state coherences in a Λ or V system was first considered by Agarwal [1974], but has received more attention recently in the context of lasing without inversion (Imamoglu [1989], Javanainen [1992], Fleischhauer, Keitel, Narducci, Scully, Zhu and Zubairy [1992]). In general the role of spontaneous emission is to erase the coherences through destructive interferences from the vacuum modes contributing to the excited state decay. However, in some particular cases those interferences do not cancel completely and a coherence may even be created by the spontaneous emission process. The most relevant case is for the Λ system when the two optical transitions $|0\rangle \rightarrow |1\rangle$ and $|0\rangle \rightarrow |2\rangle$ are completely equivalent from the point of view of the electric dipole emission, which requires two transitions at the same frequency but also with the same angular momentum quantum numbers. Javanainen [1992] considered the decay from a $|J_e = 1, m_J = 0\rangle$ level to two degenerate $|1\rangle$ and $|2\rangle$ ground levels, both of them with $J_g = 0$ quantum numbers. It is quite unlikely that such a configuration will be found in atoms, but it should not be completely excluded for molecular levels. In the case of these degenerate levels being found, the spontaneous emission terms in eq. (2.8) should be modified because of constructive interference in the upper level decay to both ground states. A new term should appear in the evolution of the ground state coherence:

$$\left.\frac{d\tilde{\rho}_{12}}{dt}\right|_{sp.em.} = \frac{\Gamma_0}{4}\rho_{00}. \tag{8.1}$$

Thus, ground-state coherence would be created in the spontaneous emission decay from the $|0\rangle$ state. Javanainen [1992] has pointed out that the superposition

principle requires the creation of that coherence. If the linear symmetric and antisymmetric combinations of ground states are considered, i.e., the coupled and noncoupled states, the upper state is dipole-connected to the coupled state only, and by spontaneous emission it will decay only to that coupled state. An atomic preparation of the coupled state through spontaneous emission implies that a coherence between the $|1\rangle$ and $|2\rangle$ ground states is formed. It is quite obvious that any experiment dealing with coherent population trapping will be affected dramatically by the presence of that coherence.

§ 9. Pulse-Matching and Photon Statistics

The research on lasing without inversion has shown that the preparation of a coherent population-trapping superposition modifies the interaction with radiation. As a consequence, properly tailored atomic superpositions may produce particular properties of the electromagnetic fields interacting with those superpositions. This section presents the application of coherent population trapping for modifying radiation field properties.

In the proposal of matched pulses by Harris [1993], a three-level system, supposed to be prepared in the $|NC\rangle$ state, was probed by a bichromatic electromagnetic field, $\mathcal{E}_{L1}(z,t)u_1\cos(\omega_{L1}t+\phi_1)$ and $\mathcal{E}_{L2}(z,t)u_2\cos(\omega_{L2}t+\phi_2)$, with time-varying envelope, applied to the two arms of a Λ system. Interacting with the $|NC\rangle$ state, the Fourier components of the input electromagnetic field, which are matched in their frequency difference, amplitude, and phase so as to preserve the atomic preparation in the noncoupled state, do not experience any absorption. On the contrary, the nonmatched Fourier components experience an absorption and are attenuated in the propagation. As a consequence, after a characteristic propagation distance, the transmitted field contains only Fourier components matched in amplitude and phase to the noncoupled state, and those components do not experience any further absorption. This concept of matched pulses has a strict connection with the observation by Dalton and Knight [1982a,b], reported in § 2.8, that critical cross-correlated fields acting on the two arms of the Λ system may preserve the coherent population-trapping preparation.

The idea of pulse matching has been formalized by the introduction of the normal modes by Harris [1994] and dressed field modes by Eberly, Pons and Haq [1994]. In effect, as the atomic time evolution is greatly simplified by using the $|NC\rangle$ state, for which eq. (2.18) expresses a time-independent evolution, a similar relation may be written for a combination of the electric field $\mathcal{E}_{L1}(z,t)$ and $\mathcal{E}_{L2}(z,t)$ components propagating through the three-level medium. The matched-

or dressed field combinations are linear combinations of the slowly varying envelopes $\mathcal{E}_{L1}(z,t)$ and $\mathcal{E}_{L2}(z,t)$, and can be derived from the Maxwell equations for propagation through the three-level system. The dressed fields represent a more general concept. If the atomic wavefunction $|\psi_g\rangle$ is written through the amplitudes a_1 and a_2 for the ground states of the Λ system:

$$|\psi_g\rangle = \frac{1}{\sqrt{|a_1|^2 + |a_2|^2}} (a_1 |1\rangle + a_2 |2\rangle), \tag{9.1}$$

the dressed-field states are defined through their Rabi frequencies Ω_C and Ω_{NC}

$$\begin{pmatrix} \Omega_C \\ \Omega_{NC} \end{pmatrix} = \begin{pmatrix} a_1 & a_2 \\ -a_2 & a_1 \end{pmatrix} \begin{pmatrix} \Omega_{R1} \\ \Omega_{R2} \end{pmatrix}, \tag{9.2}$$

where Ω_{R1} and Ω_{R2} are the Rabi frequencies for the fields acting on the $|1\rangle \rightarrow |0\rangle$ and $|2\rangle \rightarrow |0\rangle$ transitions. This linear transformation produces a coupled/noncoupled combination of the electric fields such that the Ω_C coupled field component is heavily absorbed during the propagation whereas the Ω_{NC} noncoupled field component propagates without attenuation. Under conditions of fast evolution of the excited-state population and optical coherences and of slow evolution of the ground-state coherences (fast and slow as compared to the pulse duration) the atomic amplitudes a_1 and a_2 of eq. (9.1) are determined by the initial conditions of the electric field amplitude. As a consequence, the input electric field determines the occupation amplitudes of the atomic wavefunction and fixes the linear combination Ω_{NC} of the nonattenuated electric field: the normal modes of Harris [1993] are defined by those atomic amplitudes and the Ω_C, Ω_{NC} Rabi frequencies. Normal modes may be realized in the propagation of a bichromatic pulse pair where the occupation of the coupled state is fixed through an initial interaction with the pulse pair. The pulse-pair propagation causes a distortion of the initial pulse edge and an unperturbed propagation of the remaining part of the pulse. Other methods for the preparation of the coherent trapping superposition may be also devised. Cerboneschi and Arimondo [1995] pointed out that the double-Λ scheme of fig. 26c is convenient for realizing pulse matching with great flexibility, because a pulse pair on one Λ system prepares the noncoupled superposition, whereas the pulse pair on the second Λ experiences pulse matching without any distortion of the initial edge. Notice that the definition of the dressed-field pulses by Eberly, Pons and Haq [1994] treats on the same footing the atomic superposition states and those classified as dark states in § 2.6.

Agarwal [1993] has generalized the idea of coherent population trapping by considering a quantized electromagnetic field in an approach similar to that used in the case of dressed states, but considering electromagnetic states with a very low photon number. Starting from the quantized field Hamiltonian of eq. (2.29) describing two field modes interacting with a Λ system, Agarwal searched for a wavefunction corresponding to a generalized atom–field noncoupled state, in the form of an entangled state of the atomic and field variables:

$$|\mathrm{NC_{AF}}\rangle = \mathbf{N}(g_{R2}c_1|1\rangle - g_{R1}c_2|2\rangle) \otimes |\psi_{\mathrm{field}}\rangle, \tag{9.3}$$

with the c_1 and c_2 coefficients and the $\mathbf{N}$ normalization constant to be determined. For the state $|\mathrm{NC_{AF}}\rangle$ to be an eigenvalue of the quantized Hamiltonian with zero eigenvalue, the radiation field $|\psi_{\mathrm{field}}\rangle$ wavefunction should satisfy the following equation:

$$(c_1 a_{R1} - c_2 a_{R2})|\psi_{\mathrm{field}}\rangle = 0, \tag{9.4}$$

with a_{R1} and a_{R2} the annihilation operators of the two field modes. The general solution of eq. (9.4) is obtained in terms of coherent states $|z_{R1}, z_{R2}\rangle$ associated with the two modes of the field:

$$|\psi_{\mathrm{field}}\rangle = \int q(z_{R1}) \left| z_{R1}, \frac{c_2}{c_1} z_{R1} \right\rangle \mathrm{d}z_{R1}, \tag{9.5}$$

with the c_1, c_2 coefficients and the function $q(z_{R1})$ fixed from the initial conditions of the system. The important point of this equation is that it describes two fields matched in their mode mean value:

$$\frac{\langle a_{R1}\rangle}{\langle a_{R2}\rangle} = \frac{c_1}{c_2}, \tag{9.6}$$

but also in their photon statistics, because from eq. (9.5) it results that the coherent states of the two modes are replicas of each other, only scaled by the c_1/c_2 factor.

The coherent population-trapping mechanism has determined the correlations of the two field modes. Jain [1994] has shown how the correlation in the phase noise of the two modes can be utilized for measurements limited only by the coherent-state shot noise. Agarwal, Scully and Walther [1994] have described how the ground-state coherence leads to a noise-free transfer of energy between a pump laser and a probe laser acting on the two arms of the Λ scheme. Fleischhauer [1994], investigating the correlations in the phase

fluctuations of the laser beams propagating through a three-level Λ system, pointed out the importance of the adiabatic response of the atomic coherence with respect to the phase or amplitude fluctuations of the field. In the adiabatic limit the atomic system responds promptly, and any modification in the field drives the atom into a new coherent superposition, again decoupled from the fields. In contrast, in the regime of nonadiabatic response, the atom remains in the initial noncoupled state on the time scale of the phase/amplitude field fluctuations, and those fluctuations will be damped out. In closely related papers involving the application of coherences and preparation of atoms in ground-state superpositions, the possibility of reduction of the intensity or phase noise in the three-level system has been discussed by several authors (Agarwal [1991b], Gheri and Walls [1992], Fleischhauer, Rathe and Scully [1992]). A discussion of those results will not be reported here because a clear definition of the role of coherent population trapping has not been established.

A linear superposition of ground states noncoupled to laser radiation has been considered by Cirac, Parkins, Blatt and Zoller [1993] for the motion of an ion in a trap. The ground states were associated with different vibrational states of the ionic motion. The noncoupled state formed by that superposition should present properties of squeezing in the atomic motion. Parkins, Marte, Zoller and Kimble [1993], and Parkins, Marte, Zoller, Carnal and Kimble [1995] have proposed a scheme for the preparation of general coherent superpositions of photon-number states. Three-level atoms initially in state $|1\rangle$ should experience an adiabatic transfer process, through proper time dependencies of Rabi frequencies, crossing a cavity where a laser field resonant with the transition $|1\rangle \rightarrow |0\rangle$ is present, whereas a vacuum field acts on the $|0\rangle \rightarrow |2\rangle$ transition. As a consequence of the atomic adiabatic transfer process to state $|2\rangle$, a cavity mode with one photon at frequency ω_{L2} is created. The atomic adiabatic transfer allows the generation of photons in the cavity mode starting from the laser field acting on the $|1\rangle \rightarrow |0\rangle$ transition. Sequences of atoms passing through the cavity can be used to generate Fock states of higher photon number. The adiabatic transfer from properly tailored noncoupled atomic superpositions in high-J angular momentum states allows the generation of arbitrary superpositions of Fock states.

§ 10. Conclusions

Quantum-mechanical interference effects involving the existence of two different paths for the final process are well known in laser spectroscopy investigations, and they have been fully exploited in order to improve the spectroscopy

Reprinted from

OPTICS COMMUNICATIONS

Optics Communications 127 (1996) 55–61

Matched pulses and electromagnetically induced transparency for the interaction of laser pulse pairs with a double-vee system

Elena Cerboneschi [a], Ennio Arimondo [b,1]

[a] *Dipartimento di Fisica, Università di Pisa, Piazza Torricelli 2, I-56126 Pisa, Italy*

[b] *JILA, University of Colorado, Boulder, CO 80309-0440, USA*

Received 20 September 1995; revised version received 23 January 1996; accepted 24 January 1996

N·H

ELSEVIER

ing [13]. In the DΛ scheme the coupling fields, acting on one Λ system, prepare a CPT superposition, which determines the propagation of the probe pulse pair acting on the second Λ system. However, the pulse-matching process is influenced not only by the CPT, but also by the electromagnetically induced coherence between the two upper atomic states. The contributions from CPT and quantum coherences have been identified and analyzed also in the context of lasing without inversion [14,15]. To test more precisely the role of atomic coherences in pulse matching, the propagation of pulse pairs through a four-level medium in a double-vee (DV) configuration is here investigated. In the DV scheme, the two probe pulses, taken as the candidates for pulse matching, interact with a V-type pair of transitions, where CPT cannot occur. In fact, in V-like transitions, the noncoupled state, i.e., superposition of excited states, is rapidly depopulated by spontaneous decays. On the other hand, in the DV system, the interaction of the probe pulses with the medium is affected by the coherence between the lower-energy atomic states. Here we show that such a coherence does produce pulse matching. The excitation of the lower-state coherence can be explained, again, on the basis of the CPT mechanism. Even though CPT does not take place on the pair of transitions concerned with pulse matching, it actually appears, because of the combined action of the coupling and probe fields, on other transitions of the DV system.

We show also that the space–time evolution of a pair of probe pulses, copropagating through a DV system prepared by two strong coupling fields, is governed by two normal modes. These modes describe the propagation of the pulsed excitation through the atomic medium. Our approach to normal modes is similar to that of Refs. [4] and [10], as well as to the dressed states introduced by Eberly et al. [5]. In those papers the propagation of paired fields has been examined in Λ-type systems. Our major result is that propagation normal modes have been found in the novel DV configuration. Unlike what has been done in Refs. [10] and [5], we have not applied any basis change to the atomic and field variables; instead, we have examined the space–time dependence of the atomic variables. In the hypothesis of adiabatic elimination of the atomic variables, their space dependence, equivalent to that of the field variables, allows us to determine the propagation normal modes.

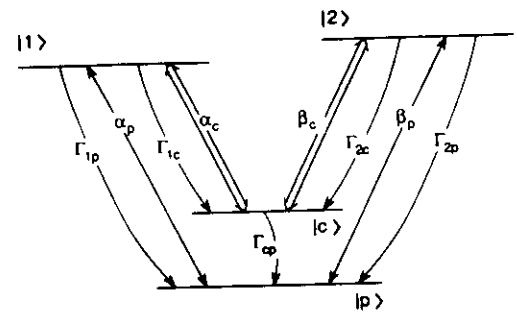

Fig. 1. Scheme of a four-level system in the DV configuration. Optical transitions and spontaneous emission decays are indicated.

In Section 2 we describe the DV scheme and discuss the atomic preparation accomplished by the coupling fields. In Section 3 the pulse matching is analyzed in the simple CPT approach and then through the normal modes. Numerical simulations supporting the analytical description are also presented.

2. DV system

As in Fig. 1, the DV scheme is composed of two pairs of V-like transitions, connecting two different low-lying states with the same pair of excited states. We consider a configuration in which two intense coupling fields interact with one of the two pairs of transitions and two weak probe pulses with the other pair. The lower eigenstates of the atomic Hamiltonian are denoted as $|p\rangle$ and $|c\rangle$ and the upper states as $|1\rangle$ and $|2\rangle$. The angular frequency separations between the upper and lower states are ω_{ij}, with $i = 1,2$ and $j = p,c$. The upper states decay by spontaneous emission into the lower states with rates Γ_{ij} $(i = 1,2, j = p,c)$. The relaxation rate from the state $|c\rangle$ into the ground state $|p\rangle$ is Γ_{cp} and the dephasing of the lower-state coherence results as $\gamma_{cp} = \Gamma_{cp}/2$.

The coupling field consists of two components resonant with the atomic transitions $|c\rangle \leftrightarrow |1\rangle$ and $|c\rangle \leftrightarrow |2\rangle$, respectively, and either field component interacts with only one transition. The coupling-field components are described by their slowly varying envelopes $E_{1c}(z,t)$ and $E_{2c}(z,t)$, z being the propagation axis of both coupling and probe lasers. The interaction with the medium is described by the space–time dependent Rabi frequencies $\alpha_c(z,t) = \mu_{1c}E_{1c}(z,t)/2\hbar$ and $\beta_c(z,t) = \mu_{2c}E_{2c}(z,t)/2\hbar$, with μ_{ij} the dipole ma-

trix element between the states $|i\rangle$ and $|j\rangle$. Analogous assumptions hold for the probe-field components, described by the Rabi frequencies $\alpha_p(z,t)$ and $\beta_p(z,t)$ associated to the transitions $|p\rangle \leftrightarrow |1\rangle$ and $|p\rangle \leftrightarrow |2\rangle$.

The Maxwell-Bloch equations form the starting point of our analysis. In the moving frame defined by the space coordinate $\zeta = z$ and the local time $\tau = t - z/c$, with c the speed of the light in the medium, the optical Bloch equations of motion for the slowly varying envelopes of the density matrix elements are (cf. those of the DΛ system [4])

$$\frac{\partial\sigma_{1p}}{\partial\tau} + \gamma_{1p}\sigma_{1p} = i\alpha_p\left(\rho_{pp} - \rho_{11}\right) - i\beta_p\sigma_{21}^* + i\alpha_c\sigma_{cp}\ , \tag{1a}$$

$$\frac{\partial\sigma_{2p}}{\partial\tau} + \gamma_{2p}\sigma_{2p} = i\beta_p\left(\rho_{pp} - \rho_{22}\right) - i\alpha_p\sigma_{21} + i\beta_c\sigma_{cp}\ , \tag{1b}$$

$$\frac{\partial\sigma_{1c}}{\partial\tau} + \gamma_{1c}\sigma_{1c} = i\alpha_c\left(\rho_{cc} - \rho_{11}\right) - i\beta_c\sigma_{21}^* + i\alpha_p\sigma_{cp}^*\ , \tag{1c}$$

$$\frac{\partial\sigma_{2c}}{\partial\tau} + \gamma_{2c}\sigma_{2c} = i\beta_c\left(\rho_{cc} - \rho_{22}\right) - i\alpha_c\sigma_{21} + i\beta_p\sigma_{cp}^*\ , \tag{1d}$$

$$\frac{\partial\sigma_{cp}}{\partial\tau} + \gamma_{cp}\sigma_{cp} = -i\alpha_p\sigma_{1c}^* - i\beta_p\sigma_{2c}^* + i\alpha_c^*\sigma_{1p} + i\beta_c^*\sigma_{2p}\ , \tag{1e}$$

$$\frac{\partial\sigma_{21}}{\partial\tau} + \gamma_{21}\sigma_{21} = i\alpha_p^*\sigma_{2p} - i\alpha_c^*\sigma_{2c} + i\beta_p\sigma_{1p}^* + i\beta_c\sigma_{1c}^*\ , \tag{1f}$$

$$\frac{\partial\rho_{pp}}{\partial\tau} = \Gamma_{1p}\rho_{11} + \Gamma_{2p}\rho_{22} + \Gamma_{cp}\rho_{cc} - 2\Im\left\{\alpha_p^*\sigma_{1p} + \beta_p^*\sigma_{2p}\right\}\ , \tag{1g}$$

$$\frac{\partial\rho_{cc}}{\partial\tau} = \Gamma_{1c}\rho_{11} + \Gamma_{2c}\rho_{22} - \Gamma_{cp}\rho_{cc} - 2\Im\left\{\alpha_c^*\sigma_{1c} + \beta_c^*\sigma_{2c}\right\}\ , \tag{1h}$$

$$\frac{\partial\rho_{11}}{\partial\tau} = -\left(\Gamma_{1p} + \Gamma_{1c}\right)\rho_{11} + 2\Im\left\{\alpha_p^*\sigma_{1p} + \alpha_c^*\sigma_{1c}\right\}\ , \tag{1i}$$

where the polarization damping rates are

$$\gamma_{1p} = \tfrac{1}{2}\left(\Gamma_{1p} + \Gamma_{1c}\right)\ , \tag{2a}$$

$$\gamma_{1c} = \tfrac{1}{2}\left(\Gamma_{1p} + \Gamma_{1c} + \Gamma_{cp}\right)\ , \tag{2b}$$

$$\gamma_{21} = \tfrac{1}{2}\sum_{l=1,2}\left(\Gamma_{lp} + \Gamma_{lc}\right)\ . \tag{2c}$$

with $i = 1,2$. In Eqs. (1a)–(1i), the equation for ρ_{22}, not included, has been eliminated through the use of the conservation of atomic occupation probability. The Maxwell equations for the slowly varying Rabi frequencies are

$$\frac{\partial\alpha_j}{\partial\zeta} = i\kappa_{1j}\sigma_{1j}\ , \tag{3a}$$

$$\frac{\partial\beta_j}{\partial\zeta} = i\kappa_{2j}\sigma_{2j}\ , \tag{3b}$$

where $j = p,c$ and the κ_{ij} coupling coefficients are, in MKS units,

$$\kappa_{ij} = \frac{\omega_{ij}N|\mu_{ij}|^2}{2c\epsilon_0\hbar}\ , \tag{4}$$

with N the atomic density of the homogeneously broadened medium [2].

The Maxwell-Bloch equations must be solved autoconsistently to determine the propagation of the laser fields. The coupling fields propagate through the medium nearly unaffected by the probe pulses, assumed much less intense. While propagating, they excite the population of the state $|c\rangle$ to the upper states $|1\rangle$ and $|2\rangle$ and, through an optical pumping process, lead population into the ground state $|p\rangle$. If the pumping rates are much larger than the ground-state relaxation rate, the pumping process is very efficient, and the whole population is pumped in $|p\rangle$. As a consequence, the coupling fields present a free propagation through the system [3]. With the whole atomic population in the ground state $|p\rangle$, the atomic polarizations σ_{1c} and σ_{2c} vanish. Eqs. (1a)–(1i) also show that, ignoring negligible terms proportional to the probe pulse amplitudes, the upper-state coherence σ_{21} drops to zero. The coupling fields are taken as pulses having, apart from the rising and falling edges, flat time profiles, as shown in Fig. 2(a). Thus the probe pulses, during their interaction time, at any position ζ, see constant coupling-field amplitudes. For what concerns the probe-field propagation, we consider

$$\rho_{pp}(\zeta,\tau) = 1\ , \tag{5a}$$

[2] When the adiabatic solution of Eq. (8a) for σ_{1p} at $\alpha_c = 0$ is substituted into the Eq. (3a) for α_p, the Beer's length $L_{B1} = \gamma_{1p}/\kappa_{1p}$ for the transition $|p\rangle \leftrightarrow |1\rangle$ is obtained.

[3] Because of the optical pumping by the coupling pulses, our whole analysis applies also to the case when $|p\rangle$ lies above $|c\rangle$.

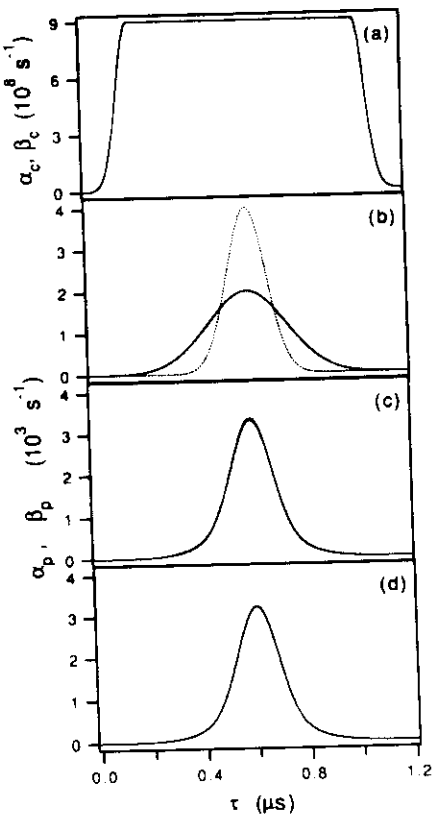

Fig. 2. Snapshots of the coupling and probe Rabi frequencies versus local time. In (a) $\alpha_c = \beta_c$ at the entry surface of the medium $\zeta = 0$. In (b) α_p (solid line) and β_p (dotted line) at $\zeta = 0$ and in (c) and (d) α_p and β_p at two different penetration depths: $\zeta = 5L_{B1}$ and $\zeta = 100L_{B1}$.

$$\rho_{cc}(\zeta,\tau) = \rho_{11}(\zeta,\tau) = \rho_{22}(\zeta,\tau) = 0\,, \tag{5b}$$

$$\sigma_{1c}(\zeta,\tau) = \sigma_{2c}(\zeta,\tau) = 0\,, \tag{5c}$$

$$\sigma_{21}(\zeta,\tau) = 0\,, \tag{5d}$$

$$\alpha_c(\zeta,\tau) = \alpha_c\,, \tag{5e}$$

$$\beta_c(\zeta,\tau) = \beta_c\,. \tag{5f}$$

3. Pulse matching

3.1. CPT approach

Fig. 1 shows that the DV system can also be seen as composed by two Λ systems sharing the same pair of lower states $|c\rangle$ and $|p\rangle$, but involving different upper states $|1\rangle$ and $|2\rangle$. For instance, the Λ system composed by the states $|c\rangle$, $|1\rangle$, and $|p\rangle$ is driven by the α_c and α_p components of the coupling and probe fields. The combined action of these two fields prepares the medium into the noncoupled state [12], defined by

$$|\mathrm{NC}_1\rangle = \frac{\alpha_c^*|p\rangle - \alpha_p^*|c\rangle}{\sqrt{|\alpha_c|^2 + |\alpha_p|^2}}\,. \tag{6}$$

It may be observed that, in the absence of the probe pulse, for $\alpha_p = 0$, the noncoupled state coincides with the optically pumped ground state $|p\rangle$. For an adiabatically smooth application of the α_p component of the probe field, the population remains in the state $|\mathrm{NC}_1\rangle$ [12]. Thus, no absorption of the α_p probe field takes place. This analysis applies, at the same time, to the second Λ system, which involves the excited state $|2\rangle$. An expression analogous to Eq. (6), with the β_p and β_c components in the place of α_p and α_c, can be written for the noncoupled state $|\mathrm{NC}_2\rangle$. The two noncoupled states coincide for $\alpha_p = \beta_p = 0$, and they must also coincide after the smooth application of the probe fields. As a consequence, the relation

$$\frac{\alpha_p}{\beta_p} = \frac{\alpha_c}{\beta_c} \tag{7}$$

must be satisfied, in the steady-state solution of the problem of the probe field interaction. Eq. (7) constitutes the definition of pulse matching in the DV system, and the same relation applies to the DΛ [13]. It shows that the shape-matched probe pulses have the same complex-amplitude ratio as the coupling fields, i.e., their amplitude ratio is determined by the preparation of the medium through the coupling pulses.

3.2. Normal modes

The normal mode analysis presented here is based on the separation of the time and space coordinates. The time dependence of the considered input pulses is very smooth. Furthermore, the time response of the atomic system is supposed to be very fast, so that, for each point in space, the steady state for the time response is reached. By using Eqs. (5a)–(5f), the density matrix equations are reduced to the following set of differential equations:

$$\frac{\partial\sigma_{1p}}{\partial\tau}(\zeta,\tau)+\gamma_{1p}\sigma_{1p}(\zeta,\tau)=i\alpha_p(\zeta,\tau)+i\alpha_c\sigma_{cp}(\zeta,\tau)\,, \tag{8a}$$

$$\frac{\partial\sigma_{2p}}{\partial\tau}(\zeta,\tau)+\gamma_{2p}\sigma_{2p}(\zeta,\tau)=i\beta_p(\zeta,\tau)+i\beta_c\sigma_{cp}(\zeta,\tau)\,, \tag{8b}$$

$$\frac{\partial\sigma_{cp}}{\partial\tau}(\zeta,\tau)+\gamma_{cp}\sigma_{cp}(\zeta,\tau)=i\alpha_c^*\sigma_{1p}(\zeta,\tau)+i\beta_c^*\sigma_{2p}(\zeta,\tau)\,. \tag{8c}$$

These equations are to be solved together with Eqs. (3a)–(3b) for α_p and β_p, in order to describe the probe-pulse propagation through the DV system prepared by the coupling pulses. If the polarization damping rates γ_{1p} and γ_{2p} are sufficiently large to allow the adiabatic elimination of the polarizations σ_{1p} and σ_{2p}, Eq. (8c) becomes

$$\frac{\partial\sigma_{cp}}{\partial\tau}(\zeta,\tau)+\left(\gamma_{cp}+\Gamma_1'+\Gamma_2'\right)\sigma_{cp}(\zeta,\tau)=-\left[\frac{\alpha_c^*}{\gamma_{1p}}\alpha_p(\zeta,\tau)+\frac{\beta_c^*}{\gamma_{2p}}\beta_p(\zeta,\tau)\right]\,, \tag{9}$$

where we have defined the optical pumping rates $\Gamma_1'=|\alpha_c|^2/\gamma_{1p}$ and $\Gamma_2'=|\beta_c|^2/\gamma_{2p}$.

The damping term on the left-hand side of this equation defines an effective decay rate for the lower-state coherence σ_{cp}, given by $\Gamma_{cp}^{\text{eff}}=\gamma_{cp}+\Gamma_1'+\Gamma_2'$. We assume the coupling-field Rabi frequencies, and therefore Γ_{cp}^{eff}, to be sufficiently large to allow the adiabatic elimination of σ_{cp}, even in the case $\gamma_{cp}=0$

$$\sigma_{cp}(\zeta,\tau)=-\frac{\alpha_c^*\alpha_p(\zeta,\tau)/\gamma_{1p}+\beta_c^*\beta_p(\zeta,\tau)/\gamma_{2p}}{\Gamma_{cp}^{\text{eff}}}\,. \tag{10}$$

By making use of Eqs. (3a)–(3b), coupled equations are derived for the space dependence of σ_{cp}, σ_{1p}, and σ_{2p}, expressing how the atomic excitation propagates through the sample. Those equations indicate that the ζ dependence of the atomic variables can be described through a linear combination of two normal modes, defined by exponentially decreasing functions. After a sufficiently long propagation through the medium, only the mode with the smaller absorption coefficient survives. Such a mode corresponds to the pulse-matching regime for the probe pulses.

The normal mode analysis is very cumbersome in the most general case, and it will be reported here for a degenerate system, with $\kappa_{1p}=\kappa_{2p}=\kappa$ and $\gamma_{1p}=\gamma_{2p}=\gamma$. In this case, the spatial evolution of the lower-state coherence and of the probe optical polarizations is given by

$$\frac{\partial\sigma_{cp}}{\partial\zeta}(\zeta,\tau)=-\frac{1}{\xi_L}\sigma_{cp}(\zeta,\tau)\,, \tag{11a}$$

$$\frac{\partial\sigma_{1p}}{\partial\zeta}(\zeta,\tau)=-\frac{1}{\xi_S}\sigma_{1p}(\zeta,\tau)-i\frac{\alpha_c}{\kappa\xi_L\xi_S}\sigma_{cp}(\zeta,\tau)\,. \tag{11b}$$

An equation similar to Eq. (11b) applies for σ_{2p}, with β_c in place of α_c. We have defined the characteristic lengths of the medium as

$$\xi_L=\frac{\gamma}{\kappa}\left[1+\frac{\Gamma_1'+\Gamma_2'}{\gamma_{cp}}\right]\,, \tag{12a}$$

$$\xi_S=\frac{\gamma}{\kappa}\,. \tag{12b}$$

The solutions of Eqs. (11a)–(11b) are

$$\sigma_{cp}(\zeta,\tau)=\sigma_{cp}(0,\tau)\exp(-\zeta/\xi_L)\,, \tag{13a}$$

$$\sigma_{1p}(\zeta,\tau)=c_1(\tau)\exp(-\zeta/\xi_S)+c_2(\tau)\exp(-\zeta/\xi_L)\,, \tag{13b}$$

with

$$c_1(\tau)=\sigma_{1p}(0,\tau)+i\frac{\alpha_c}{\kappa(\xi_L-\xi_S)}\sigma_{cp}(0,\tau)\,, \tag{14a}$$

$$c_2(\tau)=-i\frac{\alpha_c}{\kappa(\xi_L-\xi_S)}\sigma_{cp}(0,\tau)\,. \tag{14b}$$

Eqs. (13a)–(13b) show that two normal modes describe the propagation of the atomic excitation. The mode with propagation parameter ξ_S rapidly decays, since $\xi_S\ll\xi_L$ for $\Gamma_1',\Gamma_2'\gg\gamma_{cp}$. After its absorption, the following relation between σ_{1p} and σ_{cp} applies:

$$\sigma_{1p}(\zeta,\tau)=i\frac{\alpha_c}{\kappa(\xi_L-\xi_S)}\sigma_{cp}(\zeta,\tau)\,. \tag{15}$$

An analogous expression is found for the polarization σ_{2p}. The adiabatic solution of Eqs. (8a) and (8b) allows us to obtain

$$\alpha_p(\zeta,\tau)=-\alpha_c\left(1+\frac{\gamma_{cp}}{\Gamma_1'+\Gamma_2'}\right)\sigma_{cp}(\zeta,\tau)\,, \tag{16a}$$

$$\beta_p(\zeta,\tau) = -\beta_c\left(1+\frac{\gamma_{cp}}{\Gamma_1'+\Gamma_2'}\right)\sigma_{cp}(\zeta,\tau)\ . \tag{16b}$$

By dividing Eq. (16a) by Eq. (16b), the pulse-matching condition given in Eq. (7) is recovered.

We have demonstrated that the pulse matching arises from the absorption of the first normal mode, after the characteristic propagation length ξ_S. The second mode decays with the characteristic length ξ_L, which represents the transparency length for the matched pulses. Eq. (12a) shows that the transparency length ξ_L diverges when γ_{cp} approaches zero. Thus, for small γ_{cp} values matched pulses can propagate over long distances inside the medium nearly without absorption. The excitation of the lower-state coherence is responsible for pulse matching and transparency in the DV system. The dephasing of such a coherence exerts a twofold influence on the process of pulse matching. On one hand, it causes the decay of the matched pulses and therefore limits their transparency length. On the other, the analysis of the nondegenerate case shows that the coherence decay produces deviations from the pulse matching relation of Eq. (7.) Such deviations do not appear in the degenerate case presented here.

3.3. Numerical results

The analytical results have been confirmed by the numerical analysis of the Maxwell-Bloch equations. Conditions of exact resonance with the atomic transitions have been assumed, so that the amplitudes of the electromagnetic fields, assumed initially real, remain real during the propagation. In the simulations, not in the degenerate case, the parameters were similar to those of Ref. [13], with $\Gamma_{1c} = 2.6 \times 10^8$, $\Gamma_{1p} = 1.5 \times 10^8$, $\Gamma_{2c} = 3.5 \times 10^8$, $\Gamma_{2p} = 9. \times 10^7$, $\Gamma_{cp} = 1. \times 10^7$, $\omega_{1c} = 2.3 \times 10^{15}$, $\omega_{1p} = 4.7 \times 10^{15}$, $\omega_{2c} = 2.9 \times 10^{15}$, and $\omega_{2p} = 5.3 \times 10^{15}$, all of them in s^{-1}. The corresponding coupling coefficients were $\kappa_{1c} = 2.1 \times 10^7$, $\kappa_{1p} = 2.9 \times 10^6$, $\kappa_{2c} = 1.8 \times 10^7$, and $\kappa_{2p} = 1.4 \times 10^6$, all of them in $cm^{-1}\ s^{-1}$, for an atomic density $N = 10^8\ cm^{-1}$. In order to show that pulse matching takes place as described in the previous section, the decay rates have been chosen large enough to allow the adiabatic elimination of the probe-field polarizations.

The coupling-field Rabi frequencies have the initial values $\alpha_c = \beta_c = 9 \times 10^8\ s^{-1}$, in the flat central part of their time profile, as shown in Fig. 2(a). They remain unchanged during the propagation (see discussion in Section 2). Figs. 2(b–d) report the time profiles of a pair of probe pulses before entering the atomic sample, in (b), and during the propagation, at two different fixed penetration depths inside the medium, in (c) and (d). The penetration depths ζ are expressed in units of the Beer's length L_{BI} for the $|p\rangle \leftrightarrow |1\rangle$ transition (see footnote [2]). In (c), the propagation regime of pulse matching is nearly established. Since the coupling fields have been taken with the same amplitudes, the matched probe pulses are identical to each other, as from Eq. (7). As in (d), the matched pulses propagate through very long absorbing samples with negligible losses.

4. Conclusions

The propagation of a pair of weak probe pulses through a DV four-level medium prepared by two coupling fields has been examined. This configuration produces EIT with pulse matching for the probe pulses. In the DV scheme, unlike in previously studied Λ- or DΛ-type systems, CPT does not involve the pair of transitions acted upon by the coupling pulses, and a CPT state is not prepared by those pulses. Nevertheless, CPT preparation occurs through the combination of coupling and probe pulses and affects pulse matching through the excitation of the coherence between the two lower-energy states.

Under the specific conditions for the medium preparation accomplished by the coupling fields, the Maxwell-Bloch equations have been reduced to a simpler set of equations, involving only few atomic variables. With the assumption of fast decay rates for the atomic variables, those equations have been solved analytically. Two normal modes describe the propagation of the pulsed excitation through the atomic sample. The absorption of the first mode determines the reshaping of the probe pulses and leads to pulse matching. The transparency length of the matched pulses is equal to the penetration length of the less absorbed mode. This penetration length depends inversely on the dephasing rate of the lower-state coherence and, in the limit of absence of such a

dephasing, the DV medium is completely transparent for the matched pulses.

Simulations not reported here show that, when the condition for the adiabatic elimination of the atomic variables is not strictly fulfilled, the probe pulses still evolve into a pair of shape-preserving matched envelopes. However, new propagation features, such as group velocity reduction and dispersion, appear for the matched pulses.

References

[1] K.-J. Boller, A. Imamoğlu and S.E. Harris, Phys. Rev. Lett. 66 (1991) 2593.

[2] J.E. Field, K.H. Hahn and S.E. Harris, Phys. Rev. Lett. 67 (1991) 3062.

[3] S.E. Harris, J.E. Field and A. Kasapi, Phys. Rev. A 46 (1992) R29.

[4] O.A. Kocharovskaya and P. Mandel, Phys. Rev. A 42 (1990) 523.

[5] J.H. Eberly, M.L. Pons and H.R. Haq, Phys. Rev. Lett. 72 (1994) 56.

[6] R. Grobe, F.T. Hioe and J.H. Eberly, Phys. Rev. Lett. 73 (1994) 3183.

[7] A. Kasapi, M. Jain, G.Y. Yin and S.E. Harris, Phys. Rev. Lett. 74 (1994) 2447.

[8] S.E. Harris, Phys. Rev. Lett. 70 (1993) 552.

[9] G.S. Agarwal, Phys. Rev. Lett. 71 (1993) 1351.

[10] S.E. Harris, Phys. Rev. Lett. 72 (1994) 52.

[11] M. Fleischhauer, Phys. Rev. Lett. 72 (1994) 989.

[12] E. Arimondo, Progress in Optics, ed. E. Wolf (North Holland, Amsterdam, 1995) in press.

[13] E. Cerboneschi and E. Arimondo, Phys. Rev. A 52 (1995) R1823.

[14] C.H. Keitel, O. Kocharovskaya, L.M. Narducci, M.O. Scully, S.-Y. Zhu and H.M. Doss, Phys. Rev. A 48 (1993) 3196.

[15] A.S. Manka, M. Scalora, J.P. Dowling and C.M. Bowden, Optics Comm. 115 (1995) 283.

Instructions to Authors (short version)

(A more detailed version of the instructions is published in the preliminary pages of each volume)

Submission of papers

Manuscripts (one original and two copies), should be sent to one of the Editors, whose addresses are given on the inside of the journal cover.

Original material. Submission of a manuscript implies that the paper is not being simultaneously considered for publication elsewhere and that the authors have obtained the necessary authority for publication.

Refereeing. Submitted papers will be refereed and, if necessary, authors may be invited to revise their manuscript. Authors are encouraged to list the names (addresses and telephone numbers) of up to five individuals outside their institution who are qualified to serve as referees for their paper. The referees selected will not necessarily be from the list suggested by the author.

Types of contributions

The journal Optics Communications publishes short communications and full length articles in the field of optics and quantum electronics.

Short communications are brief reports of significant, original and timely research results that warrant rapid publication. The length of short communications is limited to six journal pages. Proofs will not be mailed to authors prior to publication unless specifically requested.

Full length articles are subject to the same criteria of significance and originality but give a more complete and detailed account of the research results. Proofs of all full length articles will be mailed to the corresponding author, who is requested to return the corrected version to the publisher within two days of receipt.

Manuscript preparation

All manuscripts should be written in good English. The paper copies of the text should be prepared with double line spacing and wide margins, on numbered sheets. See notes opposite on electronic version of manuscripts.

Structure. Please adhere to the following order of presentation: Article title, Author(s), Affiliation(s), Abstract, PACS codes and keywords, Main text, Acknowledgements, Appendices, References, Figure captions, Tables.

Corresponding author. The name, complete postal address, telephone and Fax numbers and the E-mail address of the corresponding author should be given on the first page of the manuscript.

PACS codes/keywords. Please supply one or more relevant PACS-1995 classification codes and 1–6 keywords of your own choice for indexing purposes.

References. References to other work should be consecutively numbered in the text using square brackets and listed by number in the Reference list. Please refer to a recent issue of the journal or to the more detailed instructions for examples.

Illustrations

Illustrations should also be submitted in triplicate: one master set and two sets of copies. The *line drawings* in the master set should be original laser printer or plotter output or drawn in black india ink, with careful lettering, large enough (3–5 mm) to remain legible after reduction for printing. The *photographs* should be originals, with somewhat more contrast than is required in the printed version. They should be unmounted unless part of a composite figure. Any scale markers should be inserted on the photograph itself, not drawn below it.

Colour plates. Figures may be published in colour, if this is judged essential by the editor. The publisher and the author will each bear part of the extra costs involved. Further information is available from the publisher.

After acceptance

Important. When page proofs are made and sent out to authors, this is in order to check that no undetected errors have arisen in the typesetting (or file conversion) process. No changes in, or additions to, the edited manuscript will be accepted.

Copyright transfer. You will be asked to transfer copyright of the article to the publisher. This transfer will ensure the widest possible dissemination of information.

Electronic manuscripts

The publisher welcomes the receipt of an electronic version of your accepted manuscript (preferably encoded in LaTex). If you have not already supplied the final, revised version of your article (on diskette) to the Journal Editor, you are requested to send a file with the text of the accepted manuscript directly to the Publisher by e-mail or on diskette (allowed formats 3.5" or 5.25" MS-DOS, or 3.5" Macintosh) to the address given below. Please note that no deviations from the version accepted by the Editor of the journal are permissible without the prior and explicit approval by the Editor. Such changes should be clearly indicated on an accompanying printout of the file.

Author benefits

No page charges. Publishing in Optics Communications is free.

Free offprints. The corresponding author will receive 50 offprints free of charge. An offprint order form will be supplied by the publisher for ordering any additional paid offprints.

Discount. Contributors to Elsevier Science journals are entitled to a 30% discount on all Elsevier Science books.

Further information (after acceptance)

Elsevier Science B.V., Optics Communication
Desk Editorial Department
P.O. Box 103, 1000 AC Amsterdam, The Netherlands
Fax: +31 20 4852319
E-mail: H. OOSTEROM@ELSEVIER.NL

PHYSICAL REVIEW A VOLUME 52, NUMBER 3 SEPTEMBER 1995

Transparency and dressing for optical pulse pairs through a double-Λ absorbing medium

Elena Cerboneschi and Ennio Arimondo
Dipartimento di Fisica, Università di Pisa, Piazza Torricelli 2, 56100 Pisa, Italy
(Received 16 November 1994)

Through numerical simulations we show that the propagation of pairs of optical pulses in a double-Λ configuration is favorable for the attainment of electromagnetically induced transparency with matched pulses, even through a long absorbing sample. The double-Λ configuration allows a flexible and precise control of the amplitudes and phases for the propagating pulses. Different atomic and field configurations based on a double-Λ system in rubidium atoms have been explored.

PACS number(s): 42.50.Gy, 42.25.Bs, 42.50.Hz

The phenomenon of electromagnetically induced transparency (EIT) in the propagation of laser radiation through an absorbing medium has been recently investigated and explained in terms of quantum coherence and interference for three-level atomic systems in Λ, V, and cascade configurations [1–5]. In the Λ configuration, if the atomic medium is prepared in a quantum superposition of states, matched pulses, i.e., a pair of optical pulses whose amplitude and phase have a well defined relation, propagate without absorption [2,4]. The mechanism of coherent population trapping [6] is responsible for EIT in a Λ system [4]. Pulse matching takes place owing to the nonlinear interaction between the pair of time-varying envelope fields and the atoms, prepared in the coherent population trapping superposition. The two fields, each one resonant with one transition of the Λ system, while propagating through the absorbing medium, experience reshaping until, after a characteristic penetration depth, temporal pulse matching of the field envelope shapes and transparency take place.

The propagation of matched pulses may be described as the spatiotemporal transparency for a linear superposition of optical electric field amplitudes. That transparent superposition of optical fields, or dressing [7], is fixed by the amplitudes in the atomic coherent trapping superposition and the preparation of the atomic quantum superposition allows a handle on the choice of the matched pulse characteristics. Thus atomic preparation represents the first stage in the realization of pulse matching. The question of the preparation of the coherent population trapping superposition state has been addressed by Agarwal [3] and Harris [4]. They assume that the time-varying fields of the pulse pair are superimposed onto constant electric field components, resonant with the atomic transitions, which produce the trapping superposition. If this assumption is renounced, numerical simulations show [4] that pulse matching is attained as well, but pulses undergo leading-edge preparation losses as they prepare the trapping state. Therefore, a completely lossless propagation cannot be achieved.

In this Rapid Communication we show, through numerical simulations, how, in a double-Λ four-level atomic system like that of Fig. 1, a separate pulse pair can be used to prepare the atomic superposition. Our numerical simulations report completely lossless propagation of shape matched pulses within long penetration distances inside an absorbing medium. Moreover, the transparency and dressing of the pulse matched pair can be controlled very precisely and with a large degree of freedom. In the double-Λ system atomic preparation and matching take place on different atomic transitions, so that a very flexible control of the amplitude and phase for the two electromagnetic fields composing the transmitted pulse is realized. The introduction of a short time delay between the preparation pulses, to be denoted as coupling, and the matched pulses, denoted as probe, allows us to separate the phases of atomic preparation and pulse matching. Furthermore, we have found that the assistance between simultaneously propagating coupling and probe pulses is responsible for an enhancement of the lossless propagation and pulse shape preserving. This electromagnetic assistance on the pulse matching is produced by the coherence between the two upper states of the four-level system. A similar electromagnetic assistance was reported before in the context of simulton theory [8].

The double-Λ scheme has already been investigated in the context of amplification without population inversion [9–11]. In [9] amplification without inversion became feasible if a high degree of coherence between the lower states was established and a definite condition on the population difference between the upper states was fulfilled. In the analysis reported in [11], the coherence between the two upper levels was shown to provide an additional mechanism for inversionless amplification. However, in our simulations we

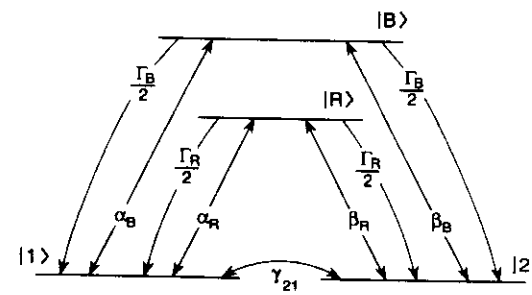

FIG. 1. Atomic energy levels in the double-Λ configuration. Optical transitions and spontaneous decays from $|B\rangle$ and $|R\rangle$ states are indicated. A nonradiative coupling γ_{21} between ground states is introduced. In the simulations, we investigated both cases with strong pulses and weak probe pulses acting on the transitions to states $|B\rangle$ and $|R\rangle$, and vice versa.

1050-2947/95/52(3)/1823(4)/$06.00

do not obtain amplification without inversion, because the characteristic requirements on the upper state populations are not fulfilled.

The double-Λ system is composed of two Λ subsystems, which share the lower energy levels $|1\rangle$ and $|2\rangle$ with upper levels $|B\rangle$ "blue" and $|R\rangle$ "red." We treat a configuration where a pair of strong coupling fields is coupled to one of the two Λ subsystems and a pair of weak probe fields interacts with the other (see Fig. 1). Since the coupling pair is several orders of magnitude stronger than the probe pair, the subsystem concerned with the coupling fields is nearly decoupled from the other. Thus the intense coupling fields trap the atoms in the nonabsorbing coherent trapping superposition of $|1\rangle$ and $|2\rangle$ ground states; the probe pulses, on the other hand, by interacting with thus prepared atoms, experience amplitude and phase shape matching. The following expressions for the applied electromagnetic fields are considered:

$$E_{R_1}(z,t)=\mathrm{Re}\{\mathscr{E}_{R_1}(z,t)\exp(-i\omega_{R_1}t+ik_{R_1}z)\},$$

$$E_{R_2}(z,t)=\mathrm{Re}\{\mathscr{E}_{R_2}(z,t)\exp(-i\omega_{R_2}t+ik_{R_2}z)\},$$

$$E_{B_1}(z,t)=\mathrm{Re}\{\mathscr{E}_{B_1}(z,t)\exp(-i\omega_{B_1}t+ik_{B_1}z)\},$$

$$E_{B_2}(z,t)=\mathrm{Re}\{\mathscr{E}_{B_2}(z,t)\exp(-i\omega_{B_2}t+ik_{B_2}z)\}, \quad (1)$$

where we assume that each field component interacts with one atomic transition only. We suppose also that exact resonance conditions are fulfilled. The time- and space-dependent Rabi frequencies, defined respectively for the transitions $|1\rangle$-$|R\rangle$ and $|2\rangle$-$|R\rangle$, are $\alpha_R=\mu_{R_1}\mathscr{E}_{R_1}/2\hbar$ and $\beta_R=\mu_{R_2}\mathscr{E}_{R_2}/2\hbar$, with μ_{R_i} $(i=1,2)$ dipole matrix elements. α_B and β_B are the analogous quantities for the transitions involving the state $|B\rangle$. If we propose using the excitations to the $|B\rangle$ state as coupling transitions, the $|NC\rangle$ noncoupled state is given by

$$|NC\rangle=\frac{\beta_B|1\rangle-\alpha_B|2\rangle}{\sqrt{\alpha_B^2+\beta_B^2}}. \quad (2)$$

$|NC\rangle$ is an eigenstate of the field-atom interaction Hamiltonian and is decoupled from the coupling fields acting on the transitions to the $|B\rangle$ state: atoms in the $|NC\rangle$ state do not absorb radiation from the coupling fields. The coupled state, given by the orthogonal superposition, allows transitions to the upper state. In general, in a double-Λ system, the $|NC\rangle$ state is nonabsorbing with respect to the coupling fields that generate it, but it does couple to the probe fields. However, if the noncoupled quantum superposition for the probe fields coincides with that of the coupling fields, the probe fields also are not absorbed and they propagate freely. It is immediately verified that the two nonabsorbing superpositions coincide if the probe pulses have their Rabi frequencies in the same ratio as the coupling pulses. The following condition results:

$$\frac{\alpha_B}{\beta_B}=\frac{\alpha_R}{\beta_R}. \quad (3)$$

Shape matched pulses satisfying this condition are stable solutions for the propagation in the double-Λ scheme. The condition of Eq. (3) is independent of which transitions of the double-Λ system are used for the coupling fields and which are used for the probe fields.

The semiclassical description of the interaction between electromagnetic fields and a homogeneously broadened material medium, in the configuration represented in Fig. 1, leads to a set of Maxwell-Bloch coupled nonlinear partial differential equations [9]. We have used, in the simulations, the parameters of a double-Λ system in a ^{87}Rb atomic beam with states [12] $|1\rangle=|5^2S_{1/2}F=1,m_F=1\rangle$, $|2\rangle=|5^2S_{1/2}F=1,m_F=-1\rangle$, $|R\rangle=|5^2P_{3/2}F=1,m_F=0\rangle$, $|B\rangle=|6^2P_{3/2}F=1,m_F=0\rangle$. The electric fields of Eq. (1) are supposed to be σ^- and σ^+ polarized. The spontaneous emission decay rates of the ^{87}Rb excited states, at wavelengths of 780.0 and 420.2 nm, respectively, are $\Gamma_R=3.77\times10^7$ s^{-1} and $\Gamma_B=8.93\times10^6$ s^{-1}. The nonradiative coupling γ_{21} between the two ground states determines the finite lifetime of the coherent trapping superposition: the value $\gamma_{21}=5\times10^4$ s^{-1} has been assumed. Such a value for γ_{21} results in a lifetime of the noncoupled state that is much longer than the time duration of the pulses, so that the loss in coherence of the ground-state superposition is not a limitation.

We have solved numerically the partial differential equations in the moving frame, along the propagation direction, defined by the variables $\zeta=z$ and retarded time $\tau=t-z/c$, where c is the velocity of the light in the medium. Given the time evolution at the entrance of the medium as an initial condition for the field envelopes, and the initial conditions of thermal equilibrium for the atomic variables throughout the medium, we determine the temporal profiles of field and atom variables at any fixed ζ position. The ζ coordinate values are expressed as multiples of α^{-1}, the Beers law absorption length for the transitions from each ground state to the excited state, which involve the probe pulses. In the simulations the amplitudes of the electromagnetic fields have been chosen real, before they enter the medium; since we assume conditions of exact resonance with the atomic transitions, they remain real during the propagation.

Figures 2 and 3 refer to the case where the coupling preparation is based on the excitations of the $|B\rangle$ state and the probe takes place on the transitions to the $|R\rangle$ state. In Fig. 2, the coupling field amplitudes are shown as a function of the time at different penetration distances through the atomic medium. They are compared with the occupations of the noncoupled trapping state and the coupled state, $\rho_{NC,NC}$ and $\rho_{C,C}$, respectively. The strong coupling blue pulses, while propagating through the medium, excite the $|B\rangle$ state and pump the atoms into the noncoupled state. In the simulations reported in Fig. 2, the maximum population in the noncoupled state is only about 90%, since the coupling fields have been switched off before the full accomplishment of the trapping process. Such a preparation of the medium does not provide the optimum conditions for pulse matching, but allows us to distinguish between different physical mechanisms concerned with pulse matching. The transmitted coupling fields, together with the population of the coupled superposition, display Rabi oscillations. The population of

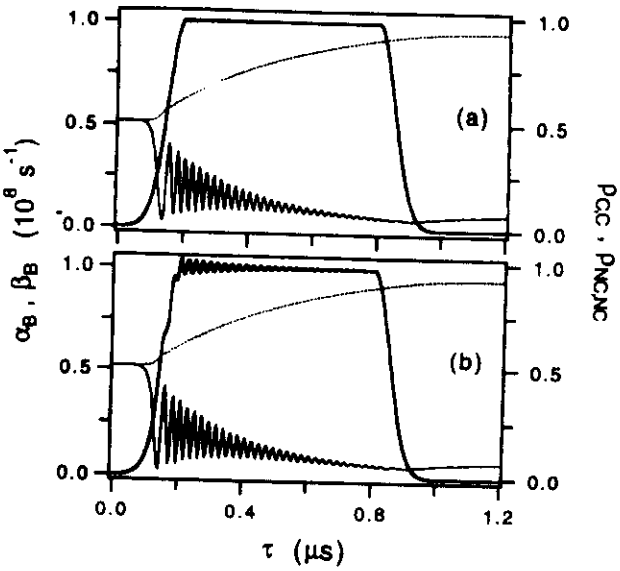

FIG. 2. Snapshots of the α_B and β_B coupling pulse amplitudes and of the occupation of the coupled and noncoupled superpositions at different penetration depths ζ through the medium. The thick solid line indicates the identical coupling amplitudes α_B and β_B with the left axis. Thin solid and dotted lines indicate the coupled $\rho_{C,C}$ and noncoupled $\rho_{NC,NC}$ occupations with the right axis. Penetration depths in (a) $\zeta\alpha=3$ and in (b) $\zeta\alpha=30$. At $\zeta\alpha=0$, α_B and β_B are as in (a), without the tiny oscillations, and $\rho_{C,C}$ and $\rho_{NC,NC}$ are equal to 0.5, their thermal equilibrium value.

the noncoupled state does not oscillate, since such a state does not interact with the fields, while it is filled by the spontaneous decay process.

We have chosen coupling blue pulses that are identical to each other to produce the noncoupled trapping superposition of Eq. (2) composed by both lower states in equal percentages. Figure 2 shows that the coupling pulses remain equal during the propagation. With such a preparation of the atomic system, from Eq. (3) we expect exact coincidence for the final amplitudes and phases of the probe pulses. As can be seen from Fig. 2, the atomic system, which interacts with the propagating coupling pulses, reproduces the same temporal behavior at any ζ position inside the medium: the curves of the populations, in Figs. 2(a) and 2(b), are almost identical to each other. Thus the system always undergoes the same atomic preparation, and constant conditions are encountered by the probe pulses. Such a stability in the preparation of the atomic medium is essential for pulse matching to take place, so that the probe pulses reach matched temporal profiles, as shown in Fig. 3. Further simulations have demonstrated that, if the noncoupled state changes in the course of the field propagation, then the matching process is inhibited.

Figure 3 reports the shape evolution of probe pulse amplitudes α_R and β_R, as they propagate through the medium, simultaneously with the coupling fields shown in Fig. 2. The input pulses, at $\zeta=0$, are different in amplitude and time duration. At a penetration depth of $\zeta\alpha=3$, pulse matching is already realized, with pulse amplitudes satisfying Eq. (3). Even though the trapping state is only partially occupied, pulse shape matching takes place. At longer propagation depths, pulse matching is not accompanied by transparency, because of the residual population in the coupled absorbing

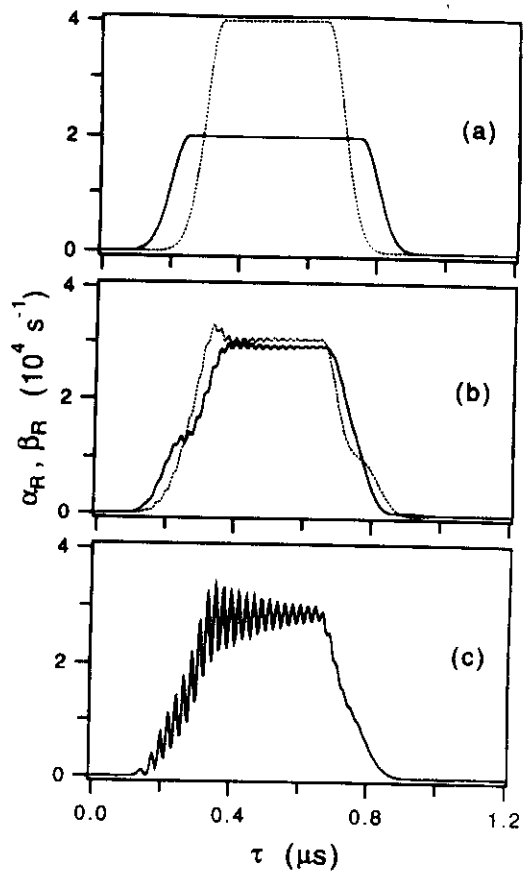

FIG. 3. Snapshots of the probe pulse amplitudes α_R (solid line) and β_R (dotted line) at different penetration depths, as they propagate simultaneously with the coupling pulses on the transitions to the $|B\rangle$ state (shown in Fig. 2). Penetration depths in (a) $\zeta\alpha=0$, in (b) $\zeta\alpha=3$, and in (c) $\zeta\alpha=30$.

state. Figure 3 evidences the presence of Rabi oscillations on the transmitted probe pulses. Those oscillations are originated by the coupling pulses on the population of the coupled state.

Figure 4 refers to a situation where the coupling fields produce a complete pumping action into the population trapping noncoupled state, so that transparency of the probe pulses remains at longer penetration depths. The atom and field parameters are the same as those of the previous cases, except that the coupling preparation takes place on the transitions to the $|R\rangle$ state and the probing stage on the transitions to the $|B\rangle$ state. This choice corresponds to the purpose of illustrating a condition with perfect dressing and transparency. A large value of Γ_R allows a faster preparation of the atoms in the trapping state. Pulse matching is reached at a penetration depth around $\zeta\alpha=10$, longer than in the case of Fig. 3. In fact, in agreement with the normal mode analyses of [4,9], the pulse matching is reached exponentially with a characteristic penetration depth that depends on the ratio between the oscillatory strength of the transition and the spontaneous decay from the upper level. Once pulse matching is realized, the penetration length where pulse matching and transparency are conserved is determined by the slow absorption of the coupling pulses. For the case of Fig. 4 (b) the transparency of the matched pulses remains at penetration

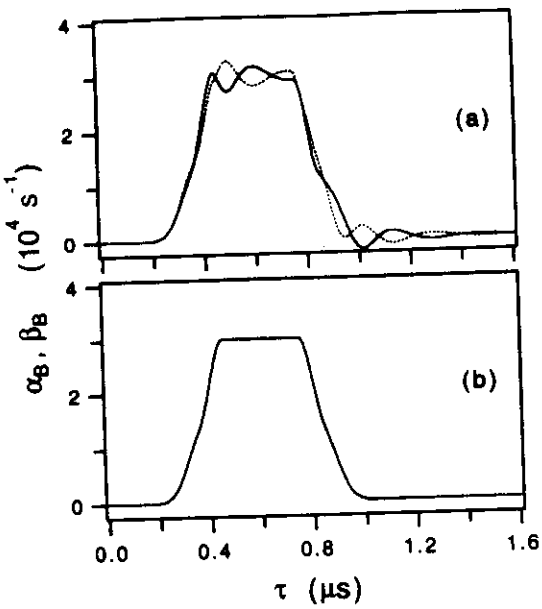

FIG. 4. Snapshots of the probe pulses α_B (solid line) and β_B (dotted line) as they propagate simultaneously with coupling lasers on the transitions to the $|R\rangle$ state. At the entrance of the medium, the probe shapes are as in Fig. 3(a). Penetration depths in (a) $\zeta\alpha = 30$ and in (b) $\zeta\alpha = 300$.

lengths longer than $\zeta\alpha = 300$. The simulations reported in Fig. 4 evidence the joint effect of the full preparation of the atoms in the trapping superposition and of the electromagnetic assistance provided by the coupling fields. The way to accomplish that is to use coupling pulses that overlap the time envelopes of the probes and propagate through the medium enough in advance to complete the trapping process.

We have also numerically investigated the pulse matching process as a function of the time delay of the probe pulses with or without time overlap with the coupling laser pulses. Without simultaneous propagation of the two pulse pairs, at time delays where the ρ_{BR} coherence has died out, but the ρ_{21} coherence is still on, the atomic system is effectively a three-level Λ system prepared in the trapping state by the coupling pair. Investigation of this time delayed regime has allowed us to isolate the influence of the coherent population trapping preparation from the electromagnetic assistance provided, through the ρ_{BR} coherence, by the simultaneous presence of the coupling fields. We have verified that, even if pulse matching is realized in the time-delayed propagation, the electromagnetic assistance greatly enhances the pulse shape preservation.

In conclusion, we have studied the propagation of pairs of weak probe pulses through a double-Λ medium, prepared by a pair of strong coupling pulses. Exploration of the pulse matching process over the different transitions of the double-Λ system has allowed us to determine the influence of different atomic and laser parameters. Numerical calculations show completely lossless propagation of shape matched pulses: leading edge preparation losses have been avoided and conditions on the pulse areas ignored. Finally the electromagnetic assistance on the pulse matching process provided by the upper level coherence has been discovered.

The authors are grateful to Professor Neal Abraham for inspiring conversations and to Dr. Marina Mazzoni for her encouraging interest in experimental realizations in this field.

[1] S. E. Harris, J. E. Field, and A. Kasapi, Phys. Rev. A **46**, R29 (1992), and references therein.
[2] S. E. Harris, Phys. Rev. Lett. **70**, 552 (1993).
[3] G. S. Agarwal, Phys. Rev. Lett. **71**, 1351 (1993).
[4] S. E. Harris, Phys. Rev. Lett. **72**, 52 (1994).
[5] A. Weis, F. Sander, and S. Kanorsky (unpublished).
[6] See A. Aspect, E. Arimondo, R. Kaiser, N. Vansteenkiste, and C. Cohen-Tannoudji, Phys. Rev. Lett. **61**, 826 (1988); J. Opt. Soc. Am. B **6**, 2112 (1989), and references therein.
[7] J. H. Eberly, M. L. Pons, and H. R. Haq, Phys. Rev. Lett. **72**, 56 (1994).
[8] M. J. Konopnicki and J. H. Eberly, Phys. Rev. A **24**, 2567 (1981).
[9] O. A. Kocharovskaya and P. Mandel, Phys. Rev. A **42**, 523 (1990).
[10] O. A. Kocharovskaya, F. Mauri, and E. Arimondo, Opt. Commun. **84**, 393 (1991).
[11] C. H. Keitel, O. A. Kocharovskaya, L. M. Narducci, M. O. Scully, S.-Y Zhu, and H. M. Doss, Phys. Rev. A **48**, 3196 (1993).
[12] The cases of degenerate or split low-lying levels lead to equivalent results for the pulse matching.

Propagation and amplitude correlation of pairs of intense pulses interacting with a double-Λ system

Elena Cerboneschi and Ennio Arimondo
Dipartimento di Fisica, Università di Pisa, Piazza Torricelli 2, I-56126 Pisa, Italy
(Received 9 July 1996)

The propagation of intense laser pulses through a four-level atomic system in a double-Λ scheme is examined. Under conditions of adiabatic perturbation of the atomic quantum state, paired pulses with arbitrary shapes establish a correlation between their amplitudes and reach a quasiform-stable regime of propagation. The amplitude correlation is a feature of pulse matching, while the propagation presents the same properties as the so-called adiabatons, predicted and observed in single-Λ systems. We show that in the double-Λ scheme the phenomena of pulse matching and adiabaton-type propagation are associated with two distinct propagation normal modes. [S1050-2947(96)07212-5]

PACS number(s): 42.50.Gy, 42.25.Bs, 42.50.Hz, 42.50.Md

I. INTRODUCTION

A Λ-type atomic medium can be pumped, by a pair of strong resonant electromagnetic fields, into a coherent superposition of the lower-energy states, where the atomic population is trapped because of destructive interferences between two different absorption paths. This phenomenon, known as coherent population trapping (CPT) [1], leads to the suppression of the total absorption of the resonant fields and renders the atomic system transparent, even with most population remaining in the lower-energy states. This type of cancellation of the absorption is currently termed electromagnetically-induced transparency (EIT). In Λ systems, the EIT is obtained as a direct consequence of the coherent trapping. In general, the EIT is produced by quantum coherences and interferences and can be achieved in different multilevel systems, including *V*-type systems where the CPT does not occur [2].

EIT has attracted much interest for its application to the amplification without inversion (AWI) [3,4] and several authors have focused their attention on the implications of the EIT on the total transmission of resonant light [5]. Dispersion properties [6] and spatial consequences [7–9] of the EIT have also been investigated, as well as applications to nonlinear optics [10]. In [11], the analysis of the phenomena of CPT, EIT, and AWI has been extended to autoionizing transitions.

The absorption and dispersion features of the EIT have important consequences on the interaction of time-dependent electromagnetic fields with an atomic medium and different aspects of the propagation of pulsed excitations through three-level systems have been discussed in several theoretical papers [12–22]. In [12], the process of pulse matching has been predicted as a result of the nonlinear interaction of two laser pulses with a Λ system, with the coherence between the lower-energy states fixed by an external preparation. This process generates a correlation between the Fourier components of the two pulses, and hence a shape matching of their temporal profiles. After the correlation is established, the matched pulses propagate without losses and without group velocity reduction and dispersion. These stable pulses can have arbitrary shape, determined by the initial pulse shapes and by the preparation conditions of the medium. As pointed out in [13], pulse matching originates by the selective absorption of a well-defined superposition of the two applied laser fields interacting with the coherently prepared Λ system, while the orthogonal superposition propagates without attenuation. The propagation of those field superpositions, termed as "dressed fields," has been discussed in [14,15], as well. Matched fields represent a steady state solution to the problem of the propagation of a pair of time-dependent fields through a Λ system. This steady state is stable against small fluctuations of the intensity and phase-difference of the two fields, as explicitly shown in [17–19]. The propagation of matched pulses in the absence of initial coherent preparation has been investigated in [13,20]. It has been shown that the preparation of the atoms is performed by the leading edge of the applied pulses, if sufficiently intense, through the CPT process, so that the atomic medium results transparent to the pulse trailing edge.

In [21], new form-stable pulses, named adiabatons, have been predicted under specific conditions of adiabatic excitation of a Λ system. The adiabatons develop as a pair of complementary pulses interacting with two different transitions and propagate with reduced group velocity. The invariance properties of this type of pulse have been discussed and specified in [22] and their essential features described experimentally in [7]. The formation of the adiabatons is understood in terms of adiabatic following of the instantaneous nonabsorbing CPT superposition and is related to the process of stimulated Raman adiabatic passage (STIRAP) [23].

Interesting propagation features have also been predicted for four-component fields interacting, in strong-coupling–weak-probe configurations, with four-level atomic systems. As shown in [24,25], these systems can be prepared coherently, by applying a pair of coupling pulses to two different atomic transitions, so that paired probe pulses, coupled to other transitions, experience shape matching and propagate without losses. Different configurations of interaction, such as the double-Λ [24] and the double-*V* [25], lead to the transparency of the four-level medium for weak probe fields. In [26], the refractive properties of the coupling-probe double-

1050-2947/96/54(6)/5400(10)/$10.00

Λ system, associated to the process of pulse matching, have been investigated.

In this work, we report on additional properties of the dynamics of the double-Λ system, when all of the driving-field components have a high intensity. We focus on the case of adiabatic perturbation of the initial coherent atomic state and use, to describe the system under these conditions, the dressed-basis representation introduced in [22]. We demonstrate, both analytically and numerically, that the adiabatons originate also in four-level systems and evidence the correlation that, in such systems, is established between the amplitudes of these pulses. Under adiabatic conditions, the field propagation is governed by two spatial normal modes. One of these modes, mainly absorptive and associated to the transient regime of pulse matching, is characterized by a short extinction length. Its absorption determines the establishment of a correlation between the amplitudes of pulses acting on different transitions. The second mode, essentially dispersive and traveling with reduced group velocity and very small losses, describes the propagation of pairs of adiabatons. Our analysis clarifies that pulse matching and adiabatons represent two distinct transient phases towards the stationary state of the atom-field system, which is represented by matched fields and coherently trapped atoms. New effects of mutual interaction between the different field components and interplay between the process of pulse matching and the formation of the adiabatons are predicted.

The organization of the paper is as follows: In Sec. II we derive the Maxwell-Bloch equations for the double-Λ system in the basis of the adiabatic dressed states. In Sec. III these equations are solved under quasiadiabatic conditions, in terms of propagation normal modes. The normal-mode solution is discussed in Sec. IV, where numerical simulations that support and extend the analytical description are also presented.

II. THE FOUR-LEVEL SYSTEM IN THE ADIABATIC DRESSED STATE BASIS

A four-level system in the double-Λ configuration is shown in the diagram of Fig. 1(a). The interaction scheme is composed by two Λ subsystems that share the lower-energy states $|1\rangle$ and $|2\rangle$. For simplicity, the dipole allowed $|1\rangle\rightarrow|i\rangle$ and $|2\rangle\rightarrow|i\rangle$ transitions ($i=c,p$) of both Λ subsystems are supposed symmetric, i.e., with equal frequency, dipole moment, and spontaneous emission rate. We describe the interaction of this system with slowly-varying four-component fields and assume that each component is only coupled to one of the allowed transitions and has its carrier frequency exactly resonant with the transition frequency. We disregard the transverse distribution of the fields and the inhomogeneous broadening of the medium. These assumptions allow us to obtain a straightforward analytical description of the spatio-temporal evolution of the system.

We indicate the angular frequency of the transitions to the upper state $|i\rangle$ ($i=c,p$) as ω_i and the natural decay rate of $|i\rangle$ as Γ_i. The population of $|i\rangle$ is supposed to decay by spontaneous emission into $|1\rangle$ and $|2\rangle$ with equal rates, given by $\Gamma_i/2$. Nonradiative decays of the lower states are neglected. A symmetric double-Λ system is provided, for instance, by two $F=1\rightarrow F=1$ atomic transitions with common lower state, driven by circularly polarized laser fields: the $m_F=1$ and $m_F=-1$ Zeeman substates of the lower state are coupled to the $m_F=0$ substate of either upper state by resonant σ^- and σ^+ field components, respectively.

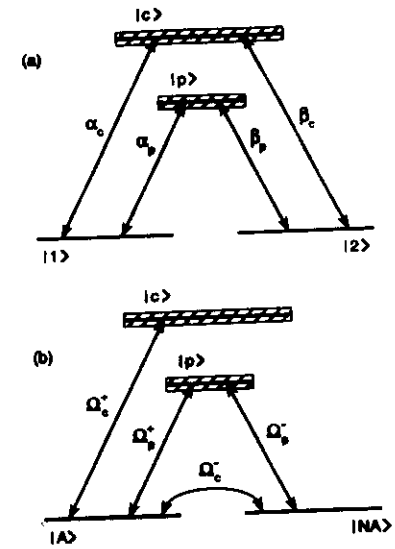

FIG. 1. Double-Λ system in the (a) bare-state and (b) dressed-state bases.

We describe the electromagnetic fields through the space-time–dependent Rabi frequencies $\alpha_c(z,t)=d_cE_{c1}(z,t)/\hbar$, $\beta_c(z,t)=d_cE_{c2}(z,t)/\hbar$, $\alpha_p(z,t)=d_pE_{p1}(z,t)/\hbar$, and $\beta_p(z,t)=d_pE_{p2}(z,t)/\hbar$, where $E_{ij}(z,t)$, for $i=c,p$ and $j=1,2$, is the slowly-varying envelope of the field component interacting with the transition $|j\rangle\rightarrow|i\rangle$ and $d_i=(3\hbar c^3\Gamma_i/8\omega_i^3)^{1/2}$ is the dipole moment matrix element of the symmetric transitions from the lower states to the upper state $|i\rangle$. The Maxwell-Bloch equations of the double-Λ system in the basis of the bare atom are written explicitly in [27]. Here we introduce the basis change to the dressed states $|NA\rangle$ and $|A\rangle$,

$$|NA\rangle=\frac{\beta_c|1\rangle-\alpha_c|2\rangle}{\sqrt{|\alpha_c|^2+|\beta_c|^2}}, \tag{1a}$$

$$|A\rangle=\frac{\alpha_c|1\rangle+\beta_c|2\rangle}{\sqrt{|\alpha_c|^2+|\beta_c|^2}}. \tag{1b}$$

If we consider $\alpha_p,\beta_p\equiv 0$, then the system in Fig. 1(a) is reduced to the Λ system composed by the states $|1\rangle$, $|2\rangle$, and $|c\rangle$: the state $|NA\rangle$ represents the nonabsorbing CPT superposition [1] associated to this system, while $|A\rangle$ is the absorbing orthogonal superposition. When the fields α_c and β_c are time dependent, unless they have matched time-profiles, $|NA\rangle$ and $|A\rangle$ are explicit functions of the time, as well. The field components α_p and β_p could be chosen as coefficients of the superpositions in Eqs. (1) in the place of α_c and β_c: the following analysis is independent of such a choice.

We describe the spatio-temporal evolution of the atom-field system in the moving frame of the coordinates $\zeta=z$ and $\tau=t-z/c$. Under exact resonance conditions, it follows from the Maxwell-Bloch equations that, if all field components are

in phase at the entry surface of the medium, and the initial atomic polarization is $\pi/2$ out of phase with respect to the field, then the phase of the field, as well as that of the atomic variables, remains unchanged during the interaction. Thus, in the following, we can assume the Rabi frequencies α_c, β_c, α_p, and β_p real for any τ and ζ. We define the new field variables $\Omega_c^{\pm}(\zeta,\tau)$ and $\Omega_p^{\pm}(\zeta,\tau)$, with dimensions of frequencies, as

$$\Omega_c^{+}(\zeta,\tau)=\sqrt{\alpha_c^2(\zeta,\tau)+\beta_c^2(\zeta,\tau)}, \tag{2a}$$

$$\Omega_c^{-}(\zeta,\tau)=\frac{\beta_c(\zeta,\tau)\frac{\partial}{\partial\tau}\alpha_c(\zeta,\tau)-\alpha_c(\zeta,\tau)\frac{\partial}{\partial\tau}\beta_c(\zeta,\tau)}{\Omega_c^{+2}(\zeta,\tau)}, \tag{2b}$$

$$\Omega_p^{+}(\zeta,\tau)=\frac{\alpha_c(\zeta,\tau)\alpha_p(\zeta,\tau)+\beta_c(\zeta,\tau)\beta_p(\zeta,\tau)}{\Omega_c^{+}(\zeta,\tau)}, \tag{2c}$$

$$\Omega_p^{-}(\zeta,\tau)=\frac{\beta_c(\zeta,\tau)\alpha_p(\zeta,\tau)-\alpha_c(\zeta,\tau)\beta_p(\zeta,\tau)}{\Omega_c^{+}(\zeta,\tau)}. \tag{2d}$$

A pair of field variables of the form of $\Omega_c^{\pm}$ has been introduced in [22] to describe the atom dynamics and the loss-free propagation of laser fields in a three-level Λ scheme under STIRAP conditions. In terms of $\Omega_c^{\pm}$ and $\Omega_p^{\pm}$, the original Rabi frequencies are expressed by

$$\alpha_c(\zeta,\tau)=\Omega_c^{+}(\zeta,\tau)\sin\left[\int_{-\infty}^{\tau}\Omega_c^{-}(\zeta,\tau')d\tau'+\text{const}\right], \tag{3a}$$

$$\beta_c(\zeta,\tau)=\Omega_c^{+}(\zeta,\tau)\cos\left[\int_{-\infty}^{\tau}\Omega_c^{-}(\zeta,\tau')d\tau'+\text{const}\right], \tag{3b}$$

$$\alpha_p(\zeta,\tau)=\frac{\alpha_c(\zeta,\tau)\Omega_p^{+}(\zeta,\tau)+\beta_c(\zeta,\tau)\Omega_p^{-}(\zeta,\tau)}{\Omega_c^{+}(\zeta,\tau)}, \tag{3c}$$

$$\beta_p(\zeta,\tau)=\frac{\beta_c(\zeta,\tau)\Omega_p^{+}(\zeta,\tau)-\alpha_c(\zeta,\tau)\Omega_p^{-}(\zeta,\tau)}{\Omega_c^{+}(\zeta,\tau)}. \tag{3d}$$

Equations (3a) and (3b) are easily obtained from the relation $\Omega_c^{-}=(d/d\tau)[\arctan(\alpha_c/\beta_c)]$, with the condition $\lim_{\tau\to-\infty}\arctan[\alpha_c(\zeta,\tau)/\beta_c(\zeta,\tau)]=\text{const}$.

In the basis of the dressed states defined in Eqs. (1), the equations for the elements of the density matrix ρ in the interaction picture read, under exact resonance conditions,

$$\frac{\partial\rho_{c(NA)}}{\partial\tau}=-\gamma_c\rho_{c(NA)}-\Omega_c^{-}\rho_{cA}-i\Omega_p^{-}\rho_{pc}+i\Omega_c^{+}\rho_{A(NA)}, \tag{4a}$$

$$\frac{\partial\rho_{cA}}{\partial\tau}=-\gamma_c\rho_{cA}-i\Omega_c^{+}(\rho_{cc}-\rho_{AA})+\Omega_c^{-}\rho_{c(NA)}-i\Omega_p^{+}\rho_{pc}, \tag{4b}$$

$$\frac{\partial\rho_{p(NA)}}{\partial\tau}=-\gamma_p\rho_{p(NA)}-i\Omega_p^{-}(\rho_{pp}-\rho_{(NA)(NA)})+i\Omega_p^{+}\rho_{A(NA)}, \tag{4c}$$

$$\frac{\partial\rho_{pA}}{\partial\tau}=-\gamma_p\rho_{pA}-i\Omega_p^{+}(\rho_{pp}-\rho_{AA})-i\Omega_c^{+}\rho_{pc}+i\Omega_p^{-}\rho_{A(NA)}, \tag{4d}$$

$$\frac{\partial\rho_{pc}}{\partial\tau}=-\gamma_{pc}\rho_{pc}-i\Omega_p^{-}\rho_{c(NA)}-i\Omega_p^{+}\rho_{cA}-i\Omega_c^{+}\rho_{pA}, \tag{4e}$$

$$\frac{\partial\rho_{A(NA)}}{\partial\tau}=\Omega_c^{-}(\rho_{(NA)(NA)}-\rho_{AA})+i\Omega_c^{+}\rho_{c(NA)}+i\Omega_p^{+}\rho_{p(NA)}+i\Omega_p^{-}\rho_{pA}, \tag{4f}$$

$$\frac{\partial\rho_{cc}}{\partial\tau}=-\Gamma_c\rho_{cc}-2i\Omega_c^{+}\rho_{cA}, \tag{4g}$$

$$\frac{\partial\rho_{pp}}{\partial\tau}=-\Gamma_p\rho_{pp}-2i(\Omega_p^{-}\rho_{p(NA)}+\Omega_p^{+}\rho_{pA}), \tag{4h}$$

$$\frac{\partial\rho_{(NA)(NA)}}{\partial\tau}=\frac{\Gamma_c}{2}\rho_{cc}+\frac{\Gamma_p}{2}\rho_{pp}+2i\Omega_p^{-}\rho_{p(NA)}-2\Omega_c^{-}\rho_{A(NA)}, \tag{4i}$$

$$\frac{\partial\rho_{AA}}{\partial\tau}=\frac{\Gamma_c}{2}\rho_{cc}+\frac{\Gamma_p}{2}\rho_{pp}+2i(\Omega_c^{+}\rho_{cA}+\Omega_p^{+}\rho_{pA})+2\Omega_c^{-}\rho_{A(NA)}, \tag{4j}$$

with

$$\gamma_c=\frac{\Gamma_c}{2}, \tag{5a}$$

$$\gamma_p=\frac{\Gamma_p}{2}, \tag{5b}$$

$$\gamma_{pc}=\frac{1}{2}(\Gamma_c+\Gamma_p). \tag{5c}$$

Here all terms proportional to the field variable Ω_c^{-} arise from the explicit dependence of $|NA\rangle$ and $|A\rangle$ on time (cf. the equations derived in [22] for the single-Λ system). Equations (4) hold for real fields. We notice that $\Omega_c^{\pm}$ and $\Omega_p^{\pm}$ can be consistently considered real if the ijth density matrix elements, with $i=A,NA$ and $j=c,p$, are considered purely imaginary and the other elements real.

Equations (4) must be solved in a self-consistent way with the Maxwell equations that, in the slowly varying envelope approximation and in terms of the field variables $\Omega_c^{\pm}$ and $\Omega_p^{\pm}$, are

$$\frac{\partial\Omega_c^{+}}{\partial\zeta}=i\kappa_c\rho_{cA}, \tag{6a}$$

$$\frac{\partial\Omega_c^{-}}{\partial\zeta}=i\kappa_c\frac{\partial}{\partial\tau}\left(\frac{\rho_{c(NA)}}{\Omega_c^{+}}\right), \tag{6b}$$

$$\frac{\partial\Omega_p^{+}}{\partial\zeta}=i\kappa_p\rho_{pA}+i\kappa_c\frac{\Omega_p^{-}}{\Omega_c^{+}}\rho_{c(NA)}, \tag{6c}$$

$$\frac{\partial \Omega_p^-}{\partial \zeta} = i\kappa_p \rho_{p(NA)} - i\kappa_c \frac{\Omega_p^+}{\Omega_c^+} \rho_{c(NA)}, \tag{6d}$$

where the coupling coefficient κ_i, for $i=c,p$, is given by

$$\kappa_i = \frac{8\pi\omega_i N |d_i|^2}{c\hbar}, \tag{7}$$

with N the atomic density.

Formally, Eqs. (4) and (6) describe a four-level system driven by the fields $\Omega_c^{\pm}$ and $\Omega_p^{\pm}$. As sketched in Fig. 1(b), Ω_c^+ and Ω_p^+ couple the state superposition $|A\rangle$ to the upper states $|c\rangle$ and $|p\rangle$, respectively, Ω_p^- couples $|NA\rangle$ to $|p\rangle$, and Ω_c^- connects $|NA\rangle$ and $|A\rangle$. Some interesting conclusions can be directly drawn from the scheme in Fig. 1(b). Let us observe that, when the original fields α_c and β_c have matched time profiles, i.e., have the same time dependence and only differ from each other by a constant scaling factor, then the transformed field Ω_c^- is identically equal to zero. On the other hand, Ω_p^- vanishes when α_p and β_p are, at any time, in the same ratio as α_c and β_c,

$$\frac{\alpha_p(\zeta,\tau)}{\beta_p(\zeta,\tau)} = \frac{\alpha_c(\zeta,\tau)}{\beta_c(\zeta,\tau)}. \tag{8}$$

When α_c and β_c have matched profiles, so that their ratio is independent of time, this equation establishes the condition of pulse matching for α_p and β_p. Provided that both Ω_c^- and Ω_p^- are equal to zero, the state superposition $|NA\rangle$ is decoupled from the fields. Then, if the atomic system is coherently prepared in $|NA\rangle$, all the population remains there indefinitely, while the transformed fields Ω_c^+ and Ω_p^+ interact with the remaining empty states and propagate freely. The conservation of Ω_c^+ and Ω_p^+ corresponds, in the bare-state representation, to the stable propagation of two pairs of matched pulses, whose amplitudes satisfy the correlation condition given in Eq. (8). Thus, in the dressed state basis it is immediately seen that pairs of arbitrarily strong and arbitrarily shaped pulses, with matched profiles and correlated amplitudes, maintain the atomic population coherently trapped in a nonabsorbing state. Atoms in the coherent trapping superposition $|NA\rangle$ and matched pulses correspond to a stationary state of the atom-field system [28].

The application of the fields Ω_c^- and Ω_p^- represents a perturbation to the stationary state described above. In this work, the spatio-temporal dynamics of the system is examined in the hypothesis of weak perturbations. This assumption does not require, in general, that the original fields α_c, β_c, α_p, and β_p are weak, since both Ω_c^- and Ω_p^- can be rendered small by properly choosing the relative amplitudes of those fields. As shown in the following, with strong original fields new nonlinear phenomena arise in the transient dynamics of the four-level system, not observed in strong-coupling–weak-probe configurations as those considered in Refs. [24–26].

III. PULSE PROPAGATION UNDER QUASIADIABATIC CONDITIONS

We now describe the transient dynamics of the atom-field system under conditions of weak coupling of the state $|NA\rangle$ to the upper states, i.e., for Ω_c^- and Ω_p^- much weaker than Ω_c^+ and Ω_p^+. When this requirement is satisfied, the evolution of the state $|NA\rangle$ is quasiadiabatic [15]. We consider, for any position ζ, the state $|NA\rangle$ fully occupied at the initial time, as an effect of a coherent preparation of the atomic sample. In fact, the double-Λ system can be prepared into any superposition of the lower-energy bare states by means of the application of a pair of sufficiently long and intense matched pulses, with proper amplitude ratio, to either Λ subsystem [20,24].

From Eqs. (4) and (6) we can see that, with all the population initially in $|NA\rangle$, Ω_c^- and Ω_p^- remain small during the interaction, if they are both small at the entry into the medium, in $\zeta=0$. For $|\Omega_c^-|,|\Omega_p^-| \ll |\Omega_c^+|,|\Omega_p^+|$, the atomic population always remains, at first order, in the state $|NA\rangle$ and the coherences between initially empty states are never excited,

$$\rho_{(NA)(NA)}(\zeta,\tau) = 1, \tag{9a}$$

$$\rho_{AA}(\zeta,\tau) = \rho_{cc}(\zeta,\tau) = \rho_{pp}(\zeta,\tau) = 0, \tag{9b}$$

$$\rho_{cA}(\zeta,\tau) = \rho_{pA}(\zeta,\tau) = \rho_{pc}(\zeta,\tau) = 0. \tag{9c}$$

Under these conditions, the equations of motion for the remaining atomic variables become

$$\frac{\partial}{\partial\tau}\rho_{c(NA)}(\zeta,\tau) = -\gamma_c \rho_{c(NA)}(\zeta,\tau) + i\Omega_c^+ \rho_{A(NA)}(\zeta,\tau), \tag{10a}$$

$$\frac{\partial}{\partial\tau}\rho_{p(NA)}(\zeta,\tau) = -\gamma_p \rho_{p(NA)}(\zeta,\tau) + i\Omega_p^-(\zeta,\tau) + i\Omega_p^+ \rho_{A(NA)}(\zeta,\tau), \tag{10b}$$

$$\frac{\partial}{\partial\tau}\rho_{A(NA)}(\zeta,\tau) = i\Omega_c^+ \rho_{c(NA)}(\zeta,\tau) + i\Omega_p^+ \rho_{p(NA)}(\zeta,\tau) + \Omega_c^-(\zeta,\tau). \tag{10c}$$

Moreover, at first order, the driving terms on the left-hand side of Eqs. (6a) and (6c) vanish, so that the fields Ω_c^+ and Ω_p^+ are conserved along ζ,

$$\Omega_c^+(\zeta,\tau) = \Omega_c^+(0,\tau), \tag{11a}$$

$$\Omega_p^+(\zeta,\tau) = \Omega_p^+(0,\tau). \tag{11b}$$

We further assume that the decay rates γ_c and γ_p are sufficiently large that the coherences $\rho_{c(NA)}$ and $\rho_{p(NA)}$ instantaneously follow the evolution of the fields. This adiabaticity hypothesis simplifies the analysis but does not change, in substance, the results presented in the following. By eliminating $\rho_{c(NA)}$ and $\rho_{p(NA)}$ from Eqs. (10a) and (10b), and substituting them in Eqs. (10c), (6b), and (6d), the Maxwell-Bloch equations are reduced to

$$\frac{\partial}{\partial\tau}\rho_{A(NA)}(\zeta,\tau)=-\left[\frac{\Omega_c^{+2}(0,\tau)}{\gamma_c}+\frac{\Omega_p^{+2}(0,\tau)}{\gamma_p}\right]\rho_{A(NA)}(\zeta,\tau)+\Omega_c^-(\zeta,\tau)-\frac{\Omega_p^+(0,\tau)}{\gamma_p}\Omega_p^-(\zeta,\tau), \quad (12a)$$

$$\frac{\partial}{\partial\zeta}\Omega_c^-(\zeta,\tau)=-\frac{\kappa_c}{\gamma_c}\frac{\partial}{\partial\tau}\rho_{A(NA)}(\zeta,\tau), \quad (12b)$$

$$\frac{\partial}{\partial\zeta}\Omega_p^-(\zeta,\tau)=-\frac{\kappa_p}{\gamma_p}\Omega_p^-(\zeta,\tau)+\left(\frac{\kappa_c}{\gamma_c}-\frac{\kappa_p}{\gamma_p}\right)\Omega_p^+(0,\tau)\rho_{A(NA)}(\zeta,\tau). \quad (12c)$$

By choosing the amplitudes of the incident fields Ω_c^+ and Ω_p^+ as constants, Eqs. (12) become a set of linear differential equations with constant coefficients, easily solved analytically in the frequency domain. This particular case allows us to determine the basic mechanisms underlying the evolution of the system.

By Fourier-transforming Eq. (12a) with respect to τ, we obtain

$$\hat{\rho}_{A(NA)}(\zeta,\omega)=\frac{1}{\Gamma_c'+\Gamma_p'-i\omega}\left[\hat{\Omega}_c^-(\zeta,\omega)-\frac{\Omega_p^+}{\gamma_p}\hat{\Omega}_p^-(\zeta,\omega)\right], \quad (13)$$

where the Fourier-transformed variables are marked by a circumflex accent and the effective decay rates $\Gamma_i'=\Omega_i^{+2}/\gamma_i$, with $i=c,p$, are introduced. By substitution of Eq. (13), the propagation equations for $\hat{\Omega}_c^-$ and $\hat{\Omega}_p^-$ become

$$\frac{\partial}{\partial\zeta}\hat{\Omega}_c^-(\zeta,\omega)=-A(\omega)\hat{\Omega}_c^-(\zeta,\omega)-B(\omega)\hat{\Omega}_p^-(\zeta,\omega), \quad (14a)$$

$$\frac{\partial}{\partial\zeta}\hat{\Omega}_p^-(\zeta,\omega)=-C(\omega)\hat{\Omega}_c^-(\zeta,\omega)-D(\omega)\hat{\Omega}_p^-(\zeta,\omega), \quad (14b)$$

with

$$A(\omega)=\eta_c^B\frac{\omega^2-i\omega(\Gamma_c'+\Gamma_p')}{\omega^2+(\Gamma_c'+\Gamma_p')^2}, \quad (15a)$$

$$B(\omega)=-\eta_c^B\frac{\omega^2-i\omega(\Gamma_c'+\Gamma_p')}{\omega^2+(\Gamma_c'+\Gamma_p')^2}\frac{\Omega_p^+}{\gamma_p}, \quad (15b)$$

$$C(\omega)=(\eta_p^B-\eta_c^B)\frac{\Gamma_c'+\Gamma_p'+i\omega}{\omega^2+(\Gamma_c'+\Gamma_p')^2}\Omega_p^+, \quad (15c)$$

$$D(\omega)=\frac{(\eta_p^B\Gamma_c'+\eta_c^B\Gamma_p')(\Gamma_c'+\Gamma_p')+\omega^2\eta_p^B-i\omega(\eta_p^B-\eta_c^B)\Gamma_p'}{\omega^2+(\Gamma_c'+\Gamma_p')^2}, \quad (15d)$$

where $\eta_i^B=\kappa_i/\gamma_i$, for $i=c,p$, denotes the Beer's absorption coefficient of the symmetric transitions from the lower states to the upper state $|i\rangle$. We notice that, if Ω_p^+ is equal to zero, or very small with respect to Ω_c^+ and to the upper state decay rates, then the coefficients B and C vanish and the evolution of $\hat{\Omega}_c^-$ and $\hat{\Omega}_p^-$ is diagonal. Thus, only for large values of Ω_p^+ a mutual interaction between the perturbation fields Ω_c^- and Ω_p^- is produced. This interaction will be discussed in the next section.

The solutions to Eqs. (14) are combinations of two normal modes $\exp\{-\eta_1\zeta\}$ and $\exp\{-\eta_2\zeta\}$,

$$\hat{\Omega}_c^-(\zeta,\omega)=a_1(\omega)e^{-\eta_1(\omega)\zeta}+a_2(\omega)e^{-\eta_2(\omega)\zeta}, \quad (16a)$$

$$\hat{\Omega}_p^-(\zeta,\omega)=b_1(\omega)e^{-\eta_1(\omega)\zeta}+b_2(\omega)e^{-\eta_2(\omega)\zeta}, \quad (16b)$$

with the propagation coefficients η_1 and η_2 satisfying the condition

$$\eta^2-(A+D)\eta+AD-BC=0. \quad (17)$$

The coefficients a_i and b_i $(i=1,2)$ are determined by imposing that $\hat{\Omega}_c^-$ and $\hat{\Omega}_p^-$ satisfy Eqs. (14) with the boundary conditions assigned in $\zeta=0$.

By solving Eq. (17), we obtain the following expressions for η_1 and η_2:

$$\eta_1=\frac{1}{2}[A+D+\sqrt{(A+D)^2-4(AD-BC)}], \quad (18a)$$

$$\eta_2=\frac{1}{2}[A+D-\sqrt{(A+D)^2-4(AD-BC)}]. \quad (18b)$$

We assume that all the relevant Fourier frequencies are sufficiently small, such that $|\omega|\ll\Gamma_c'$. At first order in ω/Γ_c', the propagation coefficients are given by

$$\eta_1\simeq\frac{1}{\zeta_1}-\frac{i\omega}{u_1}+O\left[\left(\frac{\omega}{\Gamma_c'}\right)^2\right], \quad (19a)$$

$$\eta_2\simeq-\frac{i\omega}{u_2}+O\left[\left(\frac{\omega}{\Gamma_c'}\right)^2\right], \quad (19b)$$

where the length ζ_1 and the velocity parameters u_1 and u_2 are introduced as

$$\zeta_1=\frac{\Gamma_p'+\Gamma_c'}{\eta_p^B\Gamma_c'+\eta_c^B\Gamma_p'}, \quad (20a)$$

$$u_1=\frac{(\Gamma_p'+\Gamma_c')^2}{(\eta_p^B-\eta_c^B)^2}\left(\frac{\eta_p^B}{\Gamma_p'}+\frac{\eta_c^B}{\Gamma_c'}\right), \quad (20b)$$

$$u_2=\frac{\Gamma_p'}{\eta_p^B}+\frac{\Gamma_c'}{\eta_c^B}. \quad (20c)$$

The real and imaginary parts of η_1 and η_2 represent the absorption and dispersion coefficients, respectively, associated to the two propagation normal modes. At first order $\mathcal{R}\{\eta_1\}$ is constant in ω and describes a uniform damping, with characteristic length ζ_1, of all Fourier components, while $\mathcal{I}\{\eta_1\}$ is linear in ω and determines the slowing down of the group velocity: the more Beer's coefficients η_c^B and η_p^B differ from each other, the larger this dispersive term is. For $\zeta\gg\zeta_1$ only the second mode survives. At lowest order

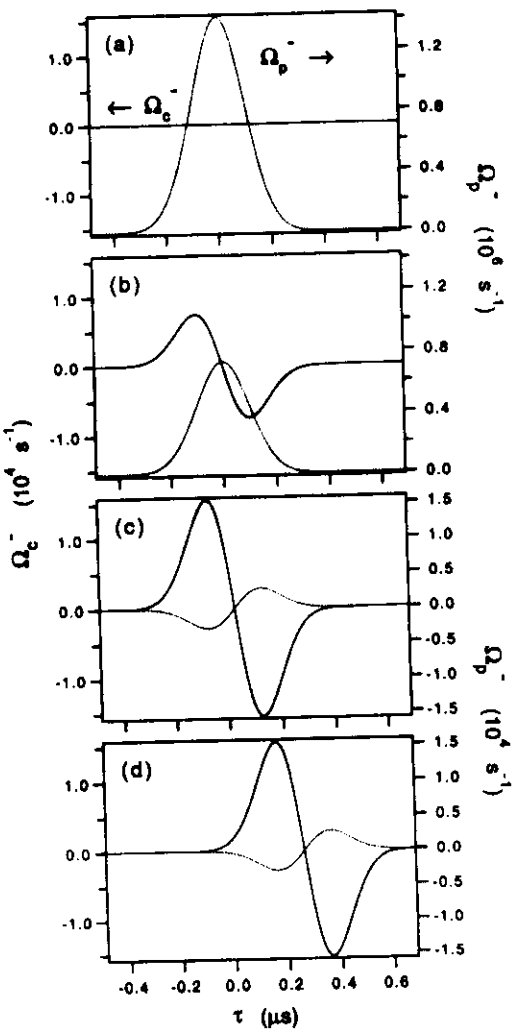

FIG. 2. Time dependence of the fields Ω_c^- (solid curves, left axes) and Ω_p^- (dotted curves, right axes) from Eqs. (21), for different penetration lengths within the medium: (a) $\zeta\eta_p^B=0$, (b) $\zeta\eta_p^B=1$, (c) $\zeta\eta_p^B=50$, and (d) $\zeta\eta_p^B=500$. The parameter values used in the calculation are $\Gamma_c=1.0\times10^8$ s^{-1}, $\Gamma_p=9.3\times10^7$ s^{-1}, $\kappa_c=3.9\times10^8$ cm^{-1} s^{-1}, $\kappa_p=1.5\times10^9$ cm^{-1} s^{-1}. For the fields Ω_c^+ and Ω_p^+ the constant value $\Omega_c^+=\Omega_p^+=1.41\times10^8$ s^{-1} has been assumed. The corresponding extinction length for the first normal mode is $\zeta_1\eta_p^B=1.51$. In (c) and (d) the scale on the right axes is expanded by two orders of magnitude with respect to (a) and (b).

η_2 is purely imaginary and linear in ω and describes a dispersive and shape-invariant propagation. In the laboratory frame, the group velocity v_i associated to the ith mode, for $i=1,2$, is defined by $1/v_i=1/c+1/u_i$. The higher-order terms in the expansions of Eqs. (19) represent nonlinear corrections to the absorption and dispersion coefficients and are responsible for small effects of group-velocity dispersion and selective absorption of high-frequency Fourier components.

IV. AMPLITUDE CORRELATION AND FORMATION OF ADIABATONS

In this section we illustrate the normal-mode solution derived above and show how it accounts for phenomena of correlation between the amplitudes of the different field components and for the formation and propagation of adiabatons. The solution is discussed, in Sec. IV A, in the dressed-atom representation, i.e., for the fields Ω_c^- and Ω_p^-, and in Sec. IV B for the original fields α_c, β_c, α_p, and β_p in the bare-atom representation. The analytical results obtained in Sec. III only apply for a limited choice of time distributions of the amplitudes of the input fields, namely, when the field variables Ω_c^+ and Ω_p^+ are independent of time. An example of time distributions that do not meet this requirement is considered in Sec. IV C. In that case, the field evolution is computed numerically, but is still understood in terms of the mechanisms previously described analytically.

A. Field evolution in the dressed-atom representation

We first use Eqs. (16) to describe the evolution of input fields $\Omega_c^-(0,\tau)$ and $\Omega_p^-(0,\tau)$ of the form shown in Fig. 2(a): $\Omega_c^-(0,\tau)$ is taken equal to zero, so that $\Omega_p^-(0,\tau)$ represents the only nonvanishing but small perturbation to the CPT steady state of the system. The fields Ω_c^+ and Ω_p^+ are assumed independent of time. For the assigned boundary conditions, the solution given in Eqs. (16), transformed back into the time domain, reads

$$\Omega_c^-(\zeta,\tau)=-\mathcal{F}\left[\frac{\partial}{\partial\tau}\Omega_p^-\left(0,\tau-\frac{\zeta}{u_1}\right)\exp\left\{-\frac{\zeta}{\zeta_1}\right\}-\frac{\partial}{\partial\tau}\Omega_p^-\left(0,\tau-\frac{\zeta}{u_2}\right)\right], \tag{21a}$$

$$\Omega_p^-(\zeta,\tau)=\Omega_p^-\left(0,\tau-\frac{\zeta}{u_1}\right)\exp\left\{-\frac{\zeta}{\zeta_1}\right\}+\mathcal{G}\left[\frac{\partial}{\partial\tau}\Omega_p^-\left(0,\tau-\frac{\zeta}{u_1}\right)\exp\left\{-\frac{\zeta}{\zeta_1}\right\}-\frac{\partial}{\partial\tau}\Omega_p^-\left(0,\tau-\frac{\zeta}{u_2}\right)\right], \tag{21b}$$

with

$$\mathcal{F}=\frac{\eta_c^B}{\eta_p^B\Gamma_c'+\eta_c^B\Gamma_p'}\frac{\Omega_p^+}{\gamma_p}, \tag{22a}$$

$$\mathcal{G}=\frac{\eta_c^B(\eta_p^B-\eta_c^B)\Gamma_p'}{(\eta_p^B\Gamma_c'+\eta_c^B\Gamma_p')^2}. \tag{22b}$$

This solution is plotted as a function of τ, for three different positions ζ, in Figs. 2(b)–2(d). For strong values of Ω_p^+, the spatial evolution of the perturbation fields Ω_c^- and Ω_p^- is determined by a combination of the two normal modes. This renders the two fields coupled to each other. For instance, in the situation examined here, we see from Eqs. (21) and from Fig. 2 that Ω_c^-, initially equal to zero, builds up from the absorption of Ω_p^- during the transient of decay of the first mode. In general, for $\zeta\gg\zeta_1$ the ratio between the fields Ω_c^- and Ω_p^- becomes independent of ζ. In the bare-atom picture this corresponds, as exemplified in Sec. IV B, to a correlation between the amplitudes of the different field components. In Figs. 2(c) and 2(d) the first propagation

mode is extinguished and the field evolution, purely determined by the second one, corresponds to a dispersive and shape-invariant propagation.

In the adiabatic limit, when the rate of change of the perturbation fields is completely negligible with respect to Ω_c^+ and Ω_p^+, Eqs. (21) simplify to $\Omega_c^-(\zeta,\tau)=0$ and $\Omega_p^-(\zeta,\tau)=\Omega_p^-(0,\tau)\exp\{-\zeta/\zeta_1\}$. This also applies when the field Ω_p^+ is negligibly small. In these cases, for $\zeta \gg \zeta_1$ both perturbation fields Ω_c^- and Ω_p^- are equal to zero so that, as shown in Sec. II, a steady propagation regime with matched pulses is established. In this sense the exponential decay of the first normal mode, with characteristic length ζ_1, corresponds to the spatial transient of pulse matching.

The second mode, corresponding to the last term on the right-hand side of both of Eqs. (21), describes the formstable and delayed propagation typical of the adiabatons, introduced in [21] for the Λ system. As first pointed out in [22], the invariance of the pulse shapes, in this kind of propagation, is an approximate result, which holds when the relevant Fourier frequencies of the perturbation fields are sufficiently small. In the present analysis, apart from the condition $|\Omega_c^-|,|\Omega_p^-| \ll |\Omega_c^+|,|\Omega_p^+|$, the shape invariance follows from the first-order truncation in the expansion of Eqs. (19). Actually, in the propagation of the adiabatons, absorption and group velocity dispersion are small effects, but not negligible over very long propagation distances. These effects cannot be observed within the distances considered in Fig. 2.

B. Field evolution in the bare-atom representation

From the solution for Ω_c^- and Ω_p^- given in Eqs. (21) and displayed in Fig. 2, by applying the formulas of Eqs. (3), we find the corresponding solution for the original fields α_c, β_c, α_p, and β_p, shown in Fig. 3. In Fig. 3(a), the fields α_c and β_c in $\zeta=0$ are independent of time and equal to each other, while, in Fig. 3(b), α_p and β_p are given by opposite-signed modulations superimposed to strong and equal continuous components: such time distributions for the original fields correspond to those of Fig. 2(a) for the transformed fields Ω_c^- and Ω_p^-, with Ω_c^+ and Ω_p^+ constant in τ. Figures 3(c) and 3(d) show that, as Ω_c^- develops at the expense of Ω_p^- [cf. Fig. 2(b)], the modulations of the incident fields α_p and β_p are transmitted to the initially flat fields α_c and β_c. In Figs. 3(e)–3(h), the behavior of the fields is shown after the first propagation mode has died out. From Eqs. (21) we see that the second mode in the evolution of both Ω_c^- and Ω_p^- is described by terms proportional to the time derivative of Ω_p^- evaluated in $\zeta=0$. In the present case, those terms are of comparable strength and, at any time τ, much smaller than the values assumed by Ω_p^- in $\zeta=0$. This appears from Figs. 2(c) and 2(d), where the fields Ω_c^- and Ω_p^- are shown after the full absorption of the first mode, when only the contribution of the second one is present: in those figures the amplitudes of Ω_c^- and Ω_p^- are two orders of magnitude smaller than the initial amplitude of Ω_p^-, in Fig. 2(a). Nevertheless, as shown in Fig. 3(e), the second mode in Ω_c^- results in a relatively strong modulation of the fields α_c and β_c, dependent on Ω_c^- through a time integral [cf. Eqs. (3a) and (3b)]. On the contrary, the second mode in Ω_p^- affects α_p and β_p very weakly. Thus, for $\zeta \gg \zeta_1$, Ω_p^- is negligible and Eq. (8) is approximately satisfied. However, that equation does not describe, here, a condition of shape matching for the fields α_p and β_p, as the ratio α_c/β_c is time dependent. Instead, it is nearly obeyed with $\alpha_c(\zeta,\tau)\approx\alpha_p(\zeta,\tau)$ and $\beta_c(\zeta,\tau)\approx\beta_p(\zeta,\tau)$. The conservation of Ω_c^+ and Ω_p^+ along ζ forces the modulations in the field pairs α_c-β_c and α_p-β_p to have opposite signs. In the bare-atom representation, the formation of modulations with complementary amplitudes in the time profiles of the fields is a feature of the adiabatons [21,22]. The comparison between the curves in Figs. 3(e) and 3(f) and those in Figs. 3(g) and 3(h) evidences that, after the absorption of the first mode, such modulations propagate simultaneously with reduced group velocity, nearly preserving their shapes for long penetration distances.

The generation of the field Ω_c^- and, in general, the coupling between the two perturbation fields can be regarded as a phenomenon of nonlinear mixing between the "pump

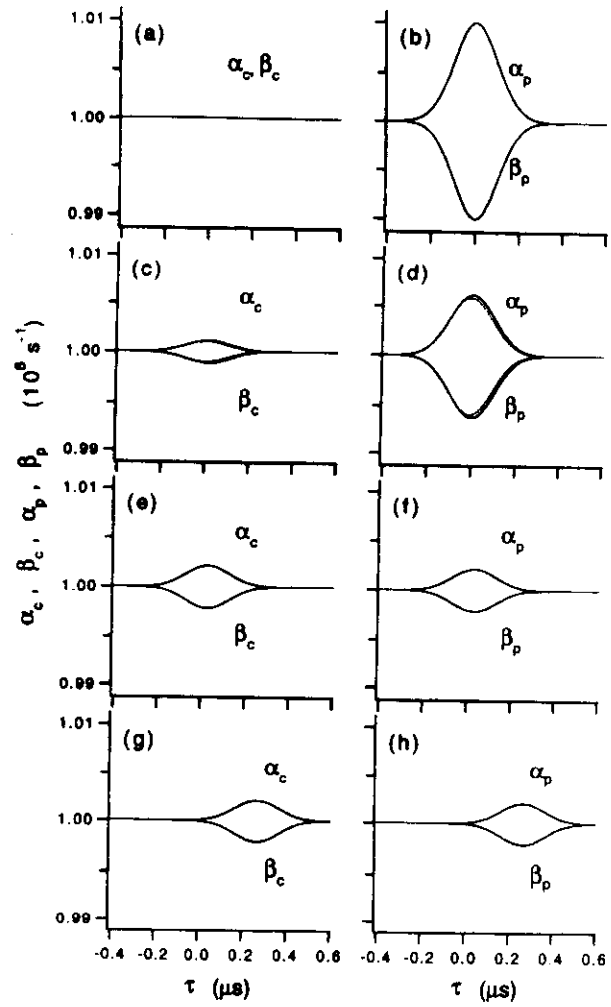

FIG. 3. Spatio-temporal evolution of the original fields α_c-β_c (left column) and α_p-β_p (right column) corresponding to that of the transformed fields Ω_c^- and Ω_p^- in Fig. 2. The time profiles of the fields are shown in (a) and (b) $\zeta\eta_p^B=0$, (c) and (d) $\zeta\eta_p^B=1$, (e) and (f) $\zeta\eta_p^B=50$, and (g) and (h) $\zeta\eta_p^B=500$. Exact numerical results (dotted curves) are shown together with the analytical results (solid curves).

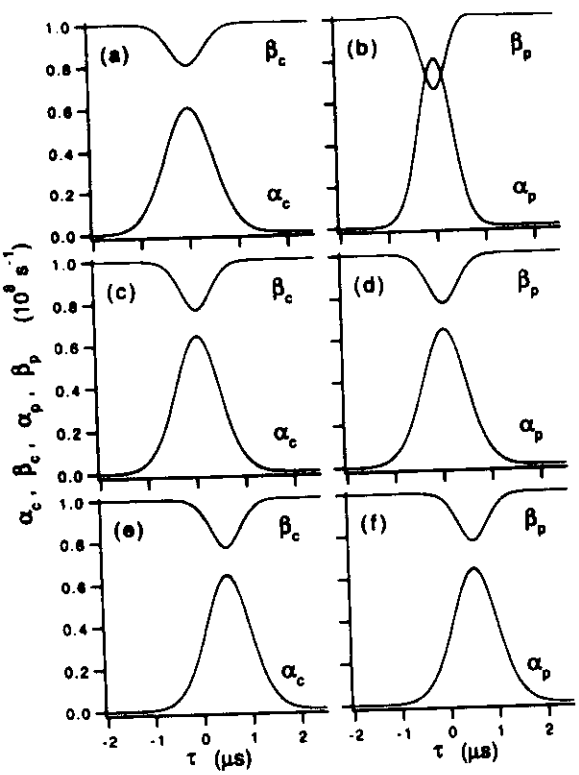

FIG. 4. Time dependence of the field pairs α_c-β_c (left column) and α_p-β_p (right column) in (a) and (b) $\zeta\eta_p^B=0$, (c) and (d) $\zeta\eta_p^B=50$, and (e) and (f) $\zeta\eta_p^B=500$. Numerical (dotted curves) and analytical (solid curves) results are almost indistinguishable. Parameters as in Fig. 3.

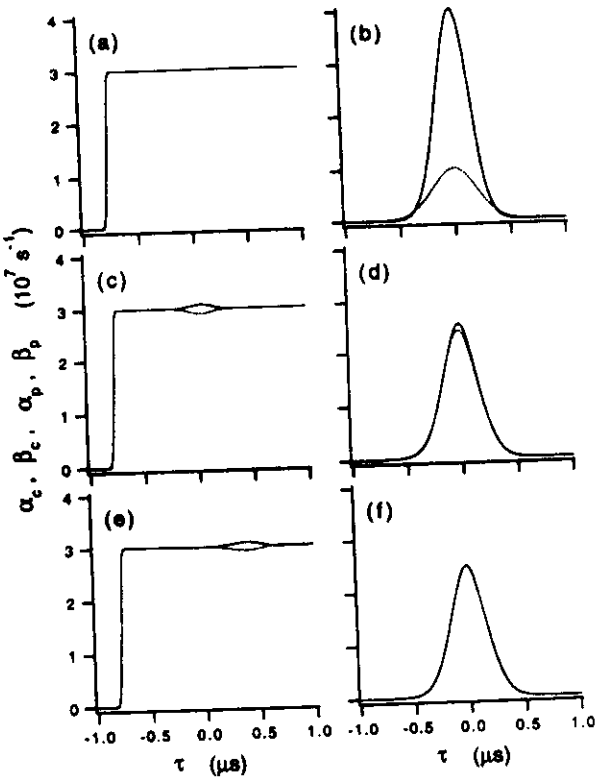

FIG. 5. Time profiles of the fields α_c, β_c (left column, solid and dotted curves, respectively), α_p, and β_p (right column, solid and dotted curves) from the numerical solution of the Maxwell-Bloch equations, at different penetration lengths: (a) and (b) $\zeta\eta_p^B=0$, (c) and (d) $\zeta\eta_p^B=50$, and (e) and (f) $\zeta\eta_p^B=500$.

waves" Ω_c^+ and Ω_p^+ and the "probe waves" Ω_c^- and Ω_p^-. In the bare-atom picture, a consequence of this mixing is the possibility to transfer amplitude modulations from one pair of fields to another. We remind the reader that, in the considered $F=1\rightarrow F=1$ interaction scheme, the field components α_c and β_c, as well as α_p and β_p, interacting with frequency-degenerate transitions from a pair of lower states to an upper state, must have an opposite circular polarization. In the situation shown in Figs. 3(a) and 3(b), α_c and β_c have flat time profiles, so that the polarization of the total field at the frequency of the transitions to the upper state $|c\rangle$ is constant in time, while the complementary modulations in the profiles of α_p and β_p correspond to a modulation in the polarization of the total field at the frequency of the transitions to the state $|p\rangle$. Thus, the adiabatons shown in Fig. 3, in the form of complementary-shaped amplitude modulations in the field pairs α_c-β_c and α_p-β_p, correspond to "polarization adiabatons" in the total fields at the two transition frequencies.

To check the validity of our approximate analysis, we have examined the evolution of the input fields shown in Figs. 3(a) and 3(b), using the whole set of Maxwell-Bloch equations. Numerical and analytical solutions, plotted together in Figs. 3(c)–3(h), show an excellent agreement.

In Figs. 4(a) and 4(b) different time distributions for the input fields in the bare-atom picture, still satisfying the conditions $\Omega_c^+(0,\tau)=\Omega_c^+(0,0)$ and $\Omega_p^+(0,\tau)=\Omega_p^+(0,0)$, are shown. With these input fields both Ω_c^- and Ω_p^- result, in $\zeta=0$, different from zero. Moreover, as the field α_c vanishes for $\tau\rightarrow-\infty$, while β_c assumes a constant value different from zero, the nonabsorbing state $|NA\rangle$ of Eq. (1a) coincides, at the beginning of the interaction, with the bare atomic state $|1\rangle$. The spatio-temporal evolution of the field amplitudes, evaluated both analytically and numerically, is illustrated in Figs. 4(c)–4(f). As noticed above, the absorption of the first propagation normal mode establishes a condition of correlation between the field components, in the form of a constant ratio between Ω_c^- and Ω_p^-. Also in this case, such a condition results in a negligibly small amplitude for Ω_p^-, compared to the amplitudes of all original fields, so that Eq. (8) is nearly satisfied, for $\zeta\gg\zeta_1$, with $\alpha_c(\zeta,\tau)\approx\alpha_p(\zeta,\tau)$ and $\beta_c(\zeta,\tau)\approx\beta_p(\zeta,\tau)$. Thus, the correlation between the field amplitudes arising from the extinction of the first mode leads again to adiabatons with approximately matched shapes.

C. Propagation of fields with a finite duration

Here we consider, in the bare-atom representation, the propagation of the input fields shown in Figs. 5(a) and 5(b). At the beginning of the interaction the field components α_c and β_c, in Fig. 5(a), are matched and, apart from their rising edge, constant in time, while α_p and β_p, in Fig. 5(b), have different time profiles and finite lengths. The analytical results derived in the preceding section do not apply in this case, since the variables Ω_c^+ and Ω_p^+ are time dependent and

the condition $|\Omega_p^-(0,\tau)| \ll |\Omega_c^+|, |\Omega_p^+|$ is not strictly fulfilled. We have calculated the evolution of the fields and the atomic variables numerically from the Maxwell-Bloch equations, with the assumption that the atoms have been prepared, for any ζ, in the pure state $|NA\rangle$. Parameter values relative to the double-Λ system formed by the states $|1\rangle = |5\,^2S_{1/2}F = 1\, m_F = 1\rangle$, $|2\rangle = |5\,^2S_{1/2}F = 1\, m_F = -1\rangle$, $|p\rangle = |5\,^2P_{3/2}F = 1\, m_F = 0\rangle$, and $|c\rangle = |6\,^2P_{3/2}F = 1\, m_F = 0\rangle$ of ^{87}Rb atoms have been assumed: $\Gamma_c = 8.93 \times 10^6$ s^{-1}, $\Gamma_p = 3.77 \times 10^7$ s^{-1}, $\omega_c = 4.5 \times 10^{15}$ s^{-1}, $\omega_p = 2.4 \times 10^{15}$ s^{-1}, and $N = 10^{10}$ cm^{-3}, corresponding to $\kappa_c = 3.74 \times 10^7$ cm^{-1} s^{-1} and $\kappa_p = 5.54 \times 10^8$ cm^{-1} s^{-1}.

To a certain extent, the situation considered here is similar to that illustrated in Fig. 3: at the entry into the medium the field variable Ω_c^- is equal to zero, α_c and β_c being identical to each other, while Ω_p^- is different from zero because of the shape mismatch between α_p and β_p. However, an important difference from the case of Fig. 3 is that here the fields α_p and β_p are taken as pulses with a finite duration, so that Ω_p^+ is different from zero only within a certain time interval. The time profiles of the field components are shown in Figs. 5(c)–5(f), for different penetration depths within the medium. Also in this case the basic mechanisms pointed out in our previous analysis govern the evolution of the system. The absorptive mode in the field propagation is rapidly extinguished. As a consequence, the mismatch between the field components α_p and β_p is strongly reduced, while modulations build up in the initially flat profiles of α_c and β_c, giving rise to a pair of complementary-shaped adiabatons. This behavior is illustrated in Figs. 5(c) and 5(d) and is analogous to that shown in Figs. 3(c) and 3(d). The remaining dispersive mode, whose group velocity is slower than the velocity c of the light in the nonresonant medium, determines the further evolution of the generated adiabatons. In terms of the transformed fields, in the dressed representation, the adiabatons typically appear, as seen in Figs. 2(c) and 2(d), as time-dependent structures, localized in time, in the profiles of the fields Ω_c^- and Ω_p^- that are, elsewhere, equal to zero. In the present case, such adiabatons accumulate longer and longer delay with respect to Ω_p^+, which has a finite length along τ and travels at velocity c. Eventually, both Ω_c^- and Ω_p^- vanish within the whole time interval of interaction of Ω_p^+. As a consequence, as predicted by the relation in Eq. (8), the original fields α_p and β_p become exactly matched in shape. Moreover, with Ω_c^- and Ω_p^- equal to zero, the fields α_p and β_p become proportional to the field variable Ω_p^+ and travel, like Ω_p^+, at velocity c without any further absorption or dispersion. On the other hand, the fields α_c and β_c, having an infinite length, can support the delayed propagation of the pair of adiabatons developed on their profiles. This situation, with a pair of matched pulses on one pair of transitions and a pair of adiabatons on the other, is depicted in Figs. 5(e) and 5(f). If the fields α_c and β_c are regarded as pulses with long but finite duration, then it turns out that the adiabatons slip through the entire length of these pulses and vanish after reaching the falling edge. Thus, finally, both of the pulse pairs α_c-β_c and α_p-β_p become matched and the CPT steady state of the atom-field system, perturbed by the initial nonzero value of the field Ω_p^-, is restored.

V. SUMMARY AND CONCLUSIONS

We have analyzed the propagation of strong resonant fields through a double-Λ four-level atomic system. We have shown that the basis of adiabatic dressed states used in [22] for the single-Λ is also convenient to describe the double-Λ system. In that basis it is immediately seen that, when both pairs of allowed transitions are driven by a pair of matched fields, then the atomic system is clamped, by CPT, in a coherent superposition of lower-energy states. Therefore, if the medium is initially prepared in such a superposition, the matched fields propagate freely at the speed of light in the nonresonant medium, and represent a stationary state for the atom-field system. Under conditions of quasiadiabatic perturbation of this steady state, the spatio-temporal evolution of the system has been investigated analytically. Our approximate analysis is confirmed by the exact numerical solution of the Maxwell-Bloch equations.

All the dynamics of the system is determined by the evolution of the field variables Ω_c^- and Ω_p^- that, in the dressed basis, represent the weak couplings of the CPT state. A perturbation approach has been used to linearize the propagation equations of such field components. Those equations are easily solved in terms of two normal modes. One of these modes, which corresponds, in the adiabatic limit, to the transient of pulse matching, is mainly absorptive and is extinguished after a relatively short penetration length of the fields inside the medium. The second mode survives the first one, because its absorption losses are very small. It describes a quasiform-stable and dispersive propagation, typical of the adiabatons and, in general, of EIT.

It may be supposed that an experimental realization of pulse propagation in media with very-many absorption lengths could be complicated due to the transverse distribution of the fields, which has been ignored throughout this work. Note, however, that the superposition $|NA\rangle$ is not dipole-connected to the excited states. As a consequence, when the population is trapped in $|NA\rangle$, saturation effects caused by the intensity-dependent atomic susceptibility, which usually arise with intense laser fields tuned near transition resonances, are eliminated [8]. Thus, the coherent trapping allows laser beams with a transverse spatial structure to propagate without distortions. In effect, an experimental demonstration that the CPT can be used for suppressing optical self-focusing and defocusing has been given in [8]. Moreover, high quality beam propagation in a CPT configuration has been reported in [7]. Nonlinear effects like bleaching and self-focusing may be important in the phase of preparation of the state $|NA\rangle$. Different methods of preparation are required, depending on the initial conditions of the atomic medium. If the population lies initially in an incoherent superposition of both states $|1\rangle$ and $|2\rangle$, then the preparation is achieved by optical pumping [24]. In this case, nonlinear distortions of the preparing fields can be minimized by rendering the characteristic time for the preparation of the superposition $|NA\rangle$ as short as possible, that is, by choosing very fast relaxation rates for the upper states. On the other hand, if all atoms are initially in a unique ground state, then the coherent trapping can be attained by employing the technique of the stimulated Raman adiabatic passage. In Refs. [7,8], it has been shown that, under STIRAP conditions, the

phase of preparation of the trapping state does not modify the transverse profile of the propagating pulses. A complete analysis of the different processes that occur during the transient of preparation, taking into account the transverse distributions of the fields, is still needed.

In conclusion, we have obtained an approximate propagation law for time-dependent fields interacting with double-Λ systems, under quasiadiabatic conditions. It includes and generalizes the description of the process of pulse matching and of the propagation of the adiabatons. Both of these phenomena have been individually studied in Λ systems, in several papers [12,13,16,19,21,22]. Our propagation law, expressed by Eqs. (14), can be easily adapted to a single-Λ system, by equating the proper field variables, along with the corresponding coupling coefficients, to zero: in this way most results derived in those papers are recovered. For instance, the well-known features of the pulse matching in the propagation of a pair of weak pulses, say α_p and β_p, through a Λ system externally prepared in a coherent superposition of lower states [13,16], can be obtained from Eqs. (14) if α_c and β_c are regarded as constant coefficients, i.e., Ω_c^- is considered identically equal to zero, and if κ_c is also taken equal to zero. On the other hand, if we consider $\Omega_p^+, \Omega_p^- \equiv 0$ and $\kappa_p = 0$, we obtain, for the propagation of adiabatons through a Λ system, the same description as in Ref. [22].

Our analysis predicts correlation phenomena, peculiar of the double-Λ system, arising from the interaction between the different field components. These phenomena take place because the evolution of the field couplings is determined by a combination of the "pulse-matching mode" and the "adiabaton-type mode."

Finally, it has been pointed out that, as concerns the polarization dynamics, the four-level schemes are more flexible and versatile than the three-level ones. The examples illustrated in Figs. 3 and 5 show that, in the double-Λ configuration, it is possible to generate a quasiform-stable modulation in the polarization of the total field at one transition frequency, by modulating the polarization of the total field at another frequency. This effect cannot be achieved in a single-Λ scheme.

ACKNOWLEDGMENTS

The authors are pleased to acknowledge stimulating discussions with N. B. Abraham and M. Fleischhauer.

[1] E. Arimondo, in *Progress in Optics*, edited by E. Wolf (North Holland, Amsterdam, 1995), Vol. 35, p. 257.
[2] M. O. Scully, Quantum Opt. **6**, 203 (1994).
[3] See, for example, O. A. Kocharovskaya and Ya. I. Khanin, Pis'ma Zh. Éksp. Teor. Fiz. **48**, 581 (1988) [JETP Lett. **48**, 630 (1988)]; S. E. Harris, Phys. Rev. Lett. **62**, 1033 (1989); M. O. Scully, S.-Y. Zhu, and A. Gavrielides, *ibid.* **62**, 2813 (1989).
[4] For experimental demonstrations of amplification and lasing without inversion, see A. S. Zibrov, M. D. Lukin, D. E. Nikonov, L. Hollberg, M. O. Scully, V. L. Velichansky, and H. G. Robinson, Phys. Rev. Lett. **75**, 1499 (1995); G. G. Padmabandu, G. R. Welch, I. N. Shubin, E. S. Fry, D. E. Nikonov, M. D. Lukin, and M. O. Scully, *ibid.* **76**, 2053 (1996), and references therein.
[5] K.-J. Boller, A. Imamoğlu, and S. E. Harris, Phys. Rev. Lett. **66**, 2593 (1991); J. E. Field, K. H. Hahn, and S. E. Harris, *ibid.* **67**, 3062 (1991); Y. Q. Li and M. Xiao, Phys. Rev. A **51**, R2703 (1995).
[6] M. O. Scully, Phys. Rev. Lett. **67**, 1855 (1991); M. Fleischhauer, C. H. Keitel, and M. O. Scully, Phys. Rev. A **46**, 1468 (1992); S. E. Harris, J. E. Field, and A. Kasapi, *ibid.* **46**, R29 (1992); M. Xiao, Y. Q. Li, S. Z. Jin, and J. Gea-Banacloche, Phys. Rev. Lett. **74**, 666 (1995); O. Schmidt, R. Wynands, Z. Hussein, and D. Meschede, Phys. Rev. A **53**, R27 (1996).
[7] A. Kasapi, M. Jain, G. Y. Yin, and S. E. Harris, Phys. Rev. Lett. **74**, 2447 (1995).
[8] M. Jain, A. J. Merriam, A. Kasapi, G. Y. Yin, and S. E. Harris, Phys. Rev. Lett. **75**, 4385 (1995).
[9] R. R. Moseley, S. Shepherd, D. J. Fulton, B. D. Sinclair, and M. H. Dunn, Phys. Rev. Lett. **74**, 670 (1995).
[10] S. E. Harris, J. E. Field, and A. Imamoğlu, Phys. Rev. Lett. **64**, 1107 (1990); K. Hakuta, L. Marmet, and B. P. Stoicheff, *ibid.* **66**, 596 (1991); R. J. Thompson, B. P. Stoicheff, G. Z. Zhang, and K. Hakuta, Quantum Opt. **6**, 349 (1994).
[11] S. J. van Enk, J. Zhang, and P. Lambropoulos, Appl. Phys. B **60**, S141 (1995).
[12] S. E. Harris, Phys. Rev. Lett. **70**, 552 (1993).
[13] S. E. Harris, Phys. Rev. Lett. **72**, 52 (1994).
[14] J. H. Eberly, M. L. Pons, and H. R. Haq, Phys. Rev. Lett. **72**, 56 (1994).
[15] J. H. Eberly, Quantum Semiclass. Opt. **7**, 373 (1995).
[16] J. H. Eberly, A. Rahman, and R. Grobe, Phys. Rev. Lett. **76**, 3687 (1996).
[17] G. S. Agarwal, Phys. Rev. Lett. **71**, 1351 (1993).
[18] M. Fleischhauer, Phys. Rev. Lett. **72**, 989 (1994).
[19] M. Fleischhauer and T. Richter, Phys. Rev. A **51**, 2430 (1995).
[20] S. E. Harris and Z.-F. Luo, Phys. Rev. A **52**, R928 (1995).
[21] R. Grobe, F. T. Hioe, and J. H. Eberly, Phys. Rev. Lett. **73**, 3183 (1994).
[22] M. Fleischhauer and A. Manka, Phys. Rev. A **54**, 794 (1996).
[23] J. Oreg, F. T. Hioe, and J. H. Eberly, Phys. Rev. A **29**, 690 (1984); J. R. Kuklinski, U. Gaubatz, F. T. Hioe, and K. Bergmann, *ibid.* **40**, 6741 (1989); M. Elk, *ibid.* **52**, 4017 (1995).
[24] E. Cerboneschi and E. Arimondo, Phys. Rev. A **52**, R1823 (1995).
[25] E. Cerboneschi and E. Arimondo, Opt. Commun. **127**, 55 (1996).
[26] I. E. Mazets (unpublished).
[27] O. A. Kocharovskaya and P. Mandel, Phys. Rev. A **42**, 523 (1990).
[28] The pulse matching is not necessarily required to satisfy the conditions $\Omega_c^-, \Omega_p^- \equiv 0$. A stationary solution is also obtained in the trivial situation when either α_c and α_p or β_c and β_p are equal to zero and the state $|NA\rangle$ coincides with one of the two low-lying states of the bare atoms.